




## Theoretical studies on structural properties and decay modes of $^{284-375}119$ isotopes

Asloob A. Rather<sup>1,2,a</sup> , M. Ikram<sup>3,b</sup>, Ishfaq A. Rather<sup>4,c</sup>, M. Imran<sup>1,d</sup>, A. A. Usmani<sup>1,e</sup>, Bharat Kumar<sup>5,f</sup>,  
K. P. Santhosh<sup>6,7,g</sup>, S. K. Patra<sup>8,h</sup>

<sup>1</sup> Department of Physics, Aligarh Muslim University, Aligarh 202002, India

<sup>2</sup> Department of School Education, Govt of Union Territory of Jammu and Kashmir, Jammu and Kashmir, India

<sup>3</sup> Department of Physics, Harsh Vidya Mandir (PG) College Raisi, Haridwar, Uttarakhand 247671, India

<sup>4</sup> Centro de Astrofísica e Gravitação-CENTRA, Instituto Superior Técnico-IST, Universidade de Lisboa-UL, Av. Rovisco Pais, Lisboa 1049-001, Portugal

<sup>5</sup> Department of Physics and Astronomy, NIT Rourkela, Odisha 769008, India

<sup>6</sup> School of Pure and Applied Physics, Kannur University, Payyanur Campus, Payyanur, Kerala 670327, India

<sup>7</sup> Department of Physics, University of Calicut, Kerala 673635, India

<sup>8</sup> Institute of Physics, Sachivalaya Marg, Bhubaneswar 751005, India

Received: 27 January 2023 / Accepted: 7 April 2023

© The Author(s), under exclusive licence to Società Italiana di Fisica and Springer-Verlag GmbH Germany, part of Springer Nature 2023

**Abstract** Within the axially deformed relativistic mean field with NL3\* parametrisation, the different bulk properties like binding energy, quadrupole deformation parameter, separation energies, density profile and shape co-existence for  $Z = 119$  isotopic chain within the mass range  $284 \leq A \leq 375$  are computed. Further, a competition between possible decay modes such as  $\alpha$ -decay,  $\beta$ -decay and spontaneous fission (SF) of the isotopic chain of  $Z = 119$  superheavy nuclei under study is systematically analysed within self-consistent relativistic mean field model and a close agreement is noticed among the calculations performed using various semi-empirical formulae and also with the estimations made by finite range droplet model (FRDM) wherever available. Our analysis confirmed that  $\alpha$ -decay is restricted within the mass range  $284 \leq A \leq 375$  and thus being the dominant decay channel in this mass range and there is no possibility of  $\beta$ -decay for the considered isotopic chain. In addition, we forecasted the  $\alpha$ -decay chain of fission survival nuclides, i.e.  $^{284-296}119$  and found as one  $\alpha$  chain from  $^{284}119$  and  $^{296}119$ ,  $2\alpha$  chains from  $^{285}119$  and  $^{295}119$  consistently,  $3\alpha$  chains from  $^{286}119$  and  $^{294}119$  consistently,  $4\alpha$  chains from  $^{287}119$  consistently, six consistent  $\alpha$  chains from  $^{288-293}119$ . A comparative study of SF and  $\alpha$ -decay half-live computed using the formula of Santhosh et al and Coulomb proximity potential model (CPPM), respectively, for the fission surviving isotopic chain reveals that isotopes  $^{288-293}119$  exhibit  $6\alpha$  chains followed by SF, isotopes  $^{295,296}119$  exhibit  $4\alpha$  chains followed by SF, and the rest of the nuclei show continuous  $\alpha$  chains. This study has also established that the alpha half-life values computed using  $Q_\alpha$  (RMF) agree with half-life values computed using experimental  $Q_\alpha$  values within 1 order difference. Thus, such studies can be of great significance to the experimentalists in very near future for synthesizing the isotopes of  $Z = 119$  superheavy nuclei.

### 1 Introduction

Theoretical and experimental studies of the nuclei with large number of neutrons and protons have witnessed an upsurge and have become the subject of intense debate among nuclear physics community from past several decades. Thus, exploring the existence limit of very heavy nuclei, i.e. nuclei with  $Z \geq 104$  and island of stability in superheavy nuclei (SHN), has been a challenging issue in nuclear physics from a fairly long period of time. The discovery of new superheavy elements (SHEs) has led to the simultaneous expansion of periodic table and Segre chart of nuclei. Hence, the studies based on the identification of new SHN would extend our knowledge about the nuclear potentials and resulting nuclear structure. The hunt for SHN started in the late 1960s with the island of stability around  $Z = 114$  and  $N = 184$  [1]. The existence of superheavy nuclei is the result of the interplay between large disruptive Coulomb force and the attractive nuclear potential. Owing to the large number of protons in SHN the Coulomb disruption dominates

<sup>a</sup> e-mail: [asloobamu@gmail.com](mailto:asloobamu@gmail.com) (corresponding author)

<sup>b</sup> e-mail: [ikramamu@gmail.com](mailto:ikramamu@gmail.com)

<sup>c</sup> e-mail: [ishfaq.rather@tecnico.ulisboa.pt](mailto:ishfaq.rather@tecnico.ulisboa.pt)

<sup>d</sup> e-mail: [imran.phys.amu@gmail.com](mailto:imran.phys.amu@gmail.com)

<sup>e</sup> e-mail: [anisul.usmani@gmail.com](mailto:anisul.usmani@gmail.com)

<sup>f</sup> e-mail: [kumarbh@nitrrkl.ac.in](mailto:kumarbh@nitrrkl.ac.in)

<sup>g</sup> e-mail: [drkpsanthosh@gmail.com](mailto:drkpsanthosh@gmail.com)

<sup>h</sup> e-mail: [patra@iopb.res.in](mailto:patra@iopb.res.in)

the attract nuclear force, thus making the SHN unstable and therefore highly susceptible to spontaneous fission. The question that arises then is what makes these SHN stable. The answer to this question came however by the end of 1960s, when it was firmly established that the existence of heavier nuclei with  $Z \geq 104$  was primarily determined by the quantum mechanical shell effects, i.e. single-particle motion of neutrons and protons in quantum orbits [2–6]. The next fundamental question that nuclear physics community try to find out is the maximum possible combination of neutrons and proton that can be found or synthesized in the laboratory. With the huge progress in theory, experiments and accelerator technologies and the advent of state-of-art radioactive ion beam facilities, it has become possible to synthesize the superheavy nuclei and reach to the island of stability in superheavy nuclei. The process of synthesizing SHN is done via fusion evaporation reactions, i.e. cold fusion reaction [7] and hot fusion reaction [8]. The cold fusion technique which involves magic spherical target and deformed projectile has been successful in synthesizing  $Z = 107 - 113$  [9–11] at GSI, Darmstadt and RIKEN, Japan. On the other hand hot fusion reaction using neutron-rich  $^{48}\text{Ca}$  beams on actinide targets, the synthesis of  $Z = 107 - 118$  has been done at JINR-FLNR, Dubna [12]. Recently in 2009, an attempt to synthesis  $Z = 120$  by using hot fusion reaction was made by Oganessian et al. [13]. However, due to the low cross-section values of the order of picobarn and sub-picobarn levels obtained in the experiments for synthesizing SHN makes the experiment to last for several months and henceforth results in the identification of few events (nuclei). Analysis of low-statistics data and investigation of new isotopes become of crucial importance. Thus, running of experiments for long periods results in optimization of production methods through the determination of excitation functions as demonstrated in recent studies of the  $^{232}\text{Am} + ^{48}\text{Ca}$  reaction [14, 15].

The elusive superheavy mass region provides an opportunity to nuclear physicists to explore the concepts like magic numbers and island of stability, which help us to understand why certain nuclei are more stable than others. Various theoretical investigations have been carried using microscopic–macroscopic approaches and the self-consistent mean field in both the relativistic and non-relativistic domains [16, 17], and the primary goal of these studies is to find out the combination of neutrons and protons where spherical shell closure may occur. However, there is no general consensus among relativistic and non-relativistic theoretical models in predicting spherical shell closures. For instance, the nuclear shell model predicts the next magic number beyond  $Z = 82$  at  $Z = 114$ . However, the microscopic–macroscopic model predicts it to be at  $Z = 114$  and  $N = 184$  [18–20] which is considered to be the island of superheavy mass region and confirmation of it has become a much debated issue nowadays. There is no confirmation till date regarding the centre of island of stability in SHN. Analogues to mic-mac predictions, the microscopic models predict closed spherical shell closures at  $N = 184$  but for nuclei with higher number of protons, i.e.  $Z = 120, 122, 124$  or  $126$  [1, 21–23]. However, it is to be noted that most of the theoretical investigations predict  $N = 184$  as the neutron magic number. The fragility/uncertainty in predicting the correct proton magic number is attributed to the ambiguous strength of spin-orbit coupling which possesses a great difficulty in localization of single-particle energy levels between  $Z = 114$  and  $126$ .

The theoretical investigations carried out specifically on  $\alpha$ -decay properties in superheavy mass have close connection to the nuclear model predictions [24–26] like clustering, shell structures, deformations and quasi-particle excitations, and various theoretical approaches have been put forth for computation of  $\alpha$ -decay properties in the superheavy mass region. One of the effective ways possibly to study SHNs is via the characterizations of their decay properties, and in particular,  $\alpha$ -decay is considered to be an inevitable tool to identify and study SHN as it provides world of information regarding the nuclear structure. The prominent mode of decay in superheavy mass region is alpha decay followed by spontaneous fission. The proper measurement of alpha decay properties provides useful inputs on structure of superheavy nuclei, for instance, shell effects and stability, nuclear spins and parities, deformation, rotational properties, fission barrier, etc. The credit to the discovery of  $\alpha$ -decay goes to Rutherford [27, 28] in 1899, and Gamow [29] was first to describe it in 1928 using the concept of quantum tunnelling through potential barrier. Currently various theoretical investigations which belong to macro–micro methods like the cluster model [30], fission model [31], the density-dependent M3Y (DDM3Y) effective model [32], the generalized liquid drop model (GLDM) [33], etc., and the self-consistent models like relativistic mean-field theory [17], Skyrme–Hartree–Fock mean field model [34] are being employed to explain the  $\alpha$ -decay from heavy and superheavy nuclei. Recently, working within the ambit of axially deformed relativistic mean field model by employing NL3\* parameterization, a systematic study of alpha decay half-lives of predicted magic nuclei  $Z = 132, 138$  [35] in the mass range  $312 \leq A \leq 392$  has been made and computation of alpha decay half-lives was performed by using the semi-empirical formulae VSS [36], Brown [37], Royer [38], GLDM [39] and Ni et al., [40]. By employing 20 mass models and 18 empirical formulae an extensive and systematic study was performed by Wang et al. [41] on alpha decay energies and alpha decay half-lives of superheavy nuclei with  $Z \geq 100$ , respectively, and established that for reproducing the  $Q_\alpha$  values of SHN, the WS4 mass model is most appropriate one. Moreover, the outcome of these studies firmly authorized that out of 18 empirical formulae SemFIS2 [42] is the most reliable one to predict alpha decay half-lives as the parameters involved in the formula are taken from experimental alpha emitter data of transuranium nuclei including SHN ( $Z = 92 - 118$ ) and the UNIV2 [42] formulae with fewest parameters are also effective in superheavy mass region. Moreover, VSS [43, 44], SP [45, 46] and NRDX [47] employing fewer parameters are also very handy in the prediction of alpha decay half-lives.

Although both alpha decay and spontaneous fission are explained by quantum mechanical tunnelling, the two widely differ in principle. Whereas alpha decay is described as the alpha cluster penetrating the Coulomb barrier after its formation in the parent nucleus, the process of spontaneous fission is much more intricate as it involves large uncertainties such as mass and charge numbers of the two fragments, the number of emitted neutrons, and the released energy. It is to be emphasized that though alpha decay and spontaneous fission are the principal modes of decay of superheavy nuclei with  $Z \geq 92$ , it the spontaneous fission that acts as limiting factor for determining the stability of superheavy nuclei. In 1939 Bohr and Wheeler [48] described the mechanism of

spontaneous fission and established a limit  $\frac{Z^2}{A} \approx 48$  for SF beyond which nuclei are susceptible to spontaneous fission. Flerov et al. [49] observed SF from  $^{238}\text{U}$ , and this was followed by several empirical formulae being proposed for determining the SF half-lives and it was Swatecki [50] in 1955 who put forward the first semi-empirical formulae for estimation of SF half-lives. Presently, we come across the globe in different laboratories [51–56] SF half-lives being measured and extensive theoretical investigations carried out by several theoretical groups for identifying the long-lived superheavy elements. Several empirical formulae have been proposed for estimation of SF fission half-lives by different researchers. Xu et al. [57] put forward a semi-empirical formula for estimating SF half-life of even–even nuclei using parabolic potential, and the agreement between theoretical and experimental results is quite good. A phenomenological formula proposed by Ren et al. [58, 59] in 2005 for calculating SF half-lives of even–even nuclei were generalized to both the case of odd nuclei and fission isomers. Within the microscopic–macroscopic model approach, Smolanczuk et al. [60] calculated the SF properties for deformed even–even, odd–A and odd–odd superheavy nuclei with  $Z = 104 - 120$ . This was followed by computation of spontaneous fission barriers of  $Z = 96 - 120$  by Muntain et al. [61] within microscopic–macroscopic model. By employing Hartree–Fock–Bogoliubov (HFB) approach with finite range and density-dependent Gogny force with the DIS parameter set Warda et al. [62] estimated the SF half-lives of 160 heavy and superheavy nuclei. The study carried out by Staszczak et al. [63] by using density functional theory for estimation of SF half-lives and life times of superheavy elements presented a systematic self-consistent approach to SF in SHN. The computation of SF half-lives using the semi-empirical formula by Ren and Xu for  $Z = 132, 138$  with mass ranges  $312 \leq A \leq 392$  and  $318 \leq A \leq 398$  has been done recently and reported in Ref. [35]. Here, in the present manuscript we made an attempt to analyse the competition among various possible modes of decay of  $Z = 119$  superheavy nuclei such as  $\alpha$ -decay,  $\beta$ -decay and SF along with the structural studies and predict the principal mode of decay of considered isotopic chain. Further, we performed the study about feasibility of observing the  $\alpha$ -decay chains for fission survival nuclides, i.e.  $^{284-297}119$  of the considered isotopic chain. The contents of the manuscript are organized as follows: The framework of relativistic mean-field formalism is outlined in section 2. Results and discussion is presented in section 3. Finally, section four contains the main summary and conclusions of this work.

## 2 The method and formalism

### 2.1 Axially deformed relativistic mean field

From the last few decades, the relativistic mean field theory has been successfully reproduced the ground state energy and other physical observables of the nuclei throughout the periodic table near as well as far from the stability line including superheavy valley [64–72]. The starting point of the RMF theory is the basic Lagrangian density containing nucleons interacting via exchange of  $\sigma$ -,  $\omega$ - and  $\rho$ -mesons. The contribution of  $\pi$ -meson is zero at mean field due to its pseudoscalar nature. Thus,  $\sigma$ -,  $\omega$ - and  $\rho$ - are only the mesonic field in which  $\sigma$ -,  $\omega$ - mesons reproduce the large scalar and vector potentials and as a result originate the reasonable nuclear mean potential and large spin-orbit potential. The  $\rho$ -meson takes the care of nuclear asymmetry of the systems. Moreover, photon field  $A_\mu$  is included to handle the Coulomb interaction between protons. The relativistic mean field Lagrangian density is expressed as [64–69],

$$\begin{aligned} \mathcal{L} = & \bar{\psi}_i \{ i \gamma^\mu \partial_\mu - M \} \psi_i + \frac{1}{2} \partial^\mu \sigma \partial_\mu \sigma - \frac{1}{2} m_\sigma^2 \sigma^2 - \frac{1}{3} g_2 \sigma^3 \\ & - \frac{1}{4} g_3 \sigma^4 - g_\sigma \bar{\psi}_i \psi_i \sigma - \frac{1}{4} \Omega^{\mu\nu} \Omega_{\mu\nu} + \frac{1}{2} m_\omega^2 V^\mu V_\mu \\ & - g_\omega \bar{\psi}_i \gamma^\mu \psi_i V_\mu - \frac{1}{4} \vec{B}^{\mu\nu} \vec{B}_{\mu\nu} + \frac{1}{2} m_\rho^2 \vec{R}^\mu \vec{R}_\mu - \frac{1}{4} F^{\mu\nu} F_{\mu\nu} \\ & - g_\rho \bar{\psi}_i \gamma^\mu \vec{\tau} \psi_i \vec{R}^\mu - e \bar{\psi}_i \gamma^\mu \frac{(1 - \tau_3 i)}{2} \psi_i A_\mu. \end{aligned} \tag{1}$$

Here  $M, m_\sigma, m_\omega$  and  $m_\rho$  are the masses for nucleon,  $\sigma$ -,  $\omega$ - and  $\rho$ -mesons and  $\psi$  is its Dirac spinor. The field for the  $\sigma$ -meson is denoted by  $\sigma$ ,  $\omega$ -meson by  $V_\mu$  and  $\rho$ -meson by  $R_\mu$ . The quantities  $g_\sigma, g_\omega, g_\rho$  and  $e^2/4\pi = 1/137$  are the coupling constants for the  $\sigma$ -,  $\omega$ -,  $\rho$ -mesons and photon field, respectively. The  $g_2$  and  $g_3$  are the nonlinear self-interaction coupling constants for  $\sigma$ -mesons. By using the classical variational principle, we obtain the field equations for the nucleons and mesons known by Dirac and Klein–Gordon equations. The Dirac equation for the nucleons is written by

$$\{ -i\alpha \nabla + V(r_\perp, z) + \beta M^\dagger \} \psi_i = \epsilon_i \psi_i. \tag{2}$$

The effective mass of the nucleon is

$$M^\dagger = M + S(r_\perp, z) = M + g_\sigma \sigma(r_\perp, z), \tag{3}$$

and the vector potential is

$$V(r_\perp, z) = g_\omega V^0(r_\perp, z) + g_\rho \tau_3 R^0(r_\perp, z) + e \frac{(1 - \tau_3)}{2} A^0(r_\perp, z). \tag{4}$$

Further, the Klein–Gordon equations are written like as

$$\{-\Delta + m_\sigma^2\}\sigma^0(r_\perp, z) = -g_\sigma \rho_s(r_\perp, z) - g_2 \sigma^2(r_\perp, z) - g_3 \sigma^3(r_\perp, z), \tag{5}$$

$$\{-\Delta + m_\omega^2\}V^0(r_\perp, z) = g_\omega \rho_v(r_\perp, z), \tag{6}$$

$$\{-\Delta + m_\rho^2\}R^0(r_\perp, z) = g_\rho \rho_3(r_\perp, z), \tag{7}$$

$$-\Delta A^0(r_\perp, z) = e\rho_c(r_\perp, z). \tag{8}$$

Here  $\rho_s(r_\perp, z)$ , and  $\rho_v(r_\perp, z)$  are the scalar and vector density for  $\sigma$ – and  $\omega$ –fields in nuclear system which are expressed as

$$\begin{aligned} \rho_s(r_\perp, z) &= \sum_{i=n,p} \bar{\psi}_i(r) \psi_i(r), \\ \rho_v(r_\perp, z) &= \sum_{i=n,p} \psi_i^\dagger(r) \psi_i(r). \end{aligned} \tag{9}$$

The vector density  $\rho_3(r_\perp, z)$  for  $\rho$ –field and charge density  $\rho_c(r_\perp, z)$  are expressed by

$$\begin{aligned} \rho_3(r_\perp, z) &= \sum_{i=n,p} \psi_i^\dagger(r) \gamma^0 \tau_{3i} \psi_i(r), \\ \rho_c(r_\perp, z) &= \sum_{i=n,p} \psi_i^\dagger(r) \gamma^0 \frac{(1 - \tau_{3i})}{2} \psi_i(r). \end{aligned} \tag{10}$$

A static solution is obtained from the equations of motion to describe the ground state properties of nuclei. The set of nonlinear coupled equations are solved self-consistently in an axially deformed harmonic oscillator basis  $N_F = N_B = 20$ , and we obtain all the physical observables. The quadrupole deformation parameter  $\beta_2$  is extracted from the calculated quadrupole moments of neutrons and protons through

$$Q = Q_n + Q_p = \sqrt{\frac{16\pi}{5}} \left( \frac{3}{4\pi} AR^2 \beta_2 \right), \tag{11}$$

where  $R = 1.2A^{1/3}$ .

The various rms radii are defined as

$$\begin{aligned} \langle r_p^2 \rangle &= \frac{1}{Z} \int r_p^2 d^3r \rho_p(r_\perp, z), \\ \langle r_n^2 \rangle &= \frac{1}{N} \int r_n^2 d^3r \rho_n(r_\perp, z), \\ \langle r_m^2 \rangle &= \frac{1}{A} \int r_m^2 d^3r \rho(r_\perp, z), \end{aligned} \tag{12}$$

for proton, neutron and matter rms radii, respectively. The quantities  $\rho_p(r_\perp, z)$ ,  $\rho_n(r_\perp, z)$  and  $\rho(r_\perp, z)$  are their corresponding densities. The charge rms radius can be found from the proton rms radius using the relation  $r_c = \sqrt{r_p^2 + 0.64}$  by taking finite size of proton into consideration. The total energy of the system is given by

$$E_{total} = E_{part} + E_\sigma + E_\omega + E_\rho + E_c + E_{pair} + E_{c.m.}, \tag{13}$$

where  $E_{part}$  is the sum of the single particle energies of the nucleons and  $E_\sigma$ ,  $E_\omega$ ,  $E_\rho$ ,  $E_c$ ,  $E_{pair}$ ,  $E_{cm}$  are the contributions of the meson fields, the Coulomb field, pairing energy and the centre-of-mass energy, respectively. In present calculations, we use the constant gap BCS approximation to take care of pairing interaction [73]. The nonlinear NL3\* parameter set [74] is used throughout the calculations.

### 2.2 Coulomb proximity potential model (CPPM)

The Coulomb proximity potential model (CPPM) [75, 76] was introduced to study alpha and cluster radioactivity and proved as an effective tool in explaining alpha decay of nuclei in superheavy region [77, 78]. The total potential in CPPM is taken as a sum of Coulomb interaction between daughter nuclei with charge number  $Z_1$  and alpha particle with charge number  $Z_2$ ; nuclear proximity potential,  $VP(z)$ ; and centrifugal potential given as:

$$V = \frac{Z_1 Z_2 e^2}{r} + V_p(z) + \frac{\hbar^2 l(l+1)}{2\mu r^2} \tag{14}$$

Here ‘ $r$ ’ is the distance between the fragment centres, ‘ $z$ ’ is the distance between the near surfaces of the fragments, ‘ $l$ ’ is the angular momentum, and ‘ $\mu$ ’ is the reduced mass.

$$V_P(z) = 4\pi\gamma b \left[ \frac{C_1 C_2}{C_1 + C_2} \right] \Phi \left( \frac{z}{b} \right) \quad (15)$$

is the proximity potential [79] with  $\gamma$  the nuclear surface tension coefficient and  $\Phi$  the universal proximity potential [80]. Here  $b \approx 1$  fermi is the diffuseness of the nuclear surface, and  $C_i$  ( $i=1,2$ ) are the Süssmann central radii of the fragments. The barrier penetrability  $P$  is given as,

$$P = \exp \left\{ -\frac{2}{\hbar} \int_a^b \sqrt{2\mu(V - Q)} dz \right\} \quad (16)$$

Using the condition,  $V(a) = V(b) = Q$ , where  $Q$  is the energy released, the turning points  $a$  and  $b$  can be determined. The decay half-life,  $T_{1/2} = \frac{\ln 2}{\lambda} = \frac{\ln 2}{\nu P}$  where  $\lambda$  is decay constant and the assault frequency,  $\nu = \frac{\omega}{2\pi} = \frac{2E_v}{\hbar}$ . The empirical vibration energy  $E_v$ , is given as [31],

$$E_v = Q \left\{ 0.056 + 0.039 \exp \left[ \frac{(4 - A_2)}{2.5} \right] \right\} \text{ for } A_2 \geq 4 \quad (17)$$

### 3 Results and discussion

It is worth mentioning that till now the superheavy nuclei up to  $Z = 118$  [81, 82] have been synthesized in the laboratory and experiments have also been attempted for the production of  $Z = 120$  [13]; however, its production cross section is very small. Thus, it is desirable to choose a proper combination of projectile and target in hot fusion reaction to improve the production cross section for magic proton shell nuclei (i.e.  $Z = 120$ ). On theoretical estimation of evaporation residue cross section, many of the possibilities of hot fusion reactions are suggested regarding the synthetization of nuclei with  $Z = 120$  [83–86]. Not only this, evaporation residue cross section for superheavy nuclei with  $Z = 119$  has also been predicted by number of nuclear physicists [84–87] and found that this nucleus might be produced easier than the magic proton shell nuclei [88]. Therefore, experiment to produce isotopes of  $Z = 119$  using hot fusion reactions is of great interest and it would bridge the gap between experimentally known  $Z = 118$  and magic proton shell nuclei. Regarding the observation of SHN, it is noticed that the superheavy nuclei are identified by  $\alpha$ -decay in the laboratory followed by spontaneous fission. In this view, it makes sense to have some theoretical predictions on decay channels of  $Z = 119$  superheavy nuclei for guiding the experiment. Concerning to this, we make mean field calculations to analyse the competition among  $\alpha$ -decay,  $\beta$ -decay and spontaneous fission for predicting the possible mode of decay of isotopic chain under study and this is considered to be central theme of the paper. In addition to gain some structural information, we calculate the total binding energy (BE), radii, quadrupole deformation parameter ( $\beta_2$ ) and density profile for three possible shape configurations in the mass range of  $284 \leq A \leq 375$  which covers many of the neutron magic numbers. The results concerning to structure and decay of  $Z = 119$  isotopic chain are fully explained in subsections 3.1 to 3.5.

#### 3.1 Binding energy, radii and quadrupole deformation parameter

The calculated binding energy, radii and quadrupole deformation parameter for the isotopic chain  $^{284-375}_{119}$  are given in Tables 1 and plotted in Figs. 1, 2. To identify the possible ground state configuration of the nuclei, the field equations are solved with an initial spherical, prolate and oblate quadrupole deformation parameter  $\beta_0$  in relativistic mean field formalism. Nucleus, a quantum many body system, acquires different binding energy by their possible shape configurations leading to the ground as well as intrinsic excited states. It is worthy to mention that maximum binding energy of a quantum system corresponds to the ground state energy of the system and all other solutions may correspond to the intrinsic excited states. Concerning these facts into consideration, we found prolate as a ground state for most of the nuclides of  $Z = 119$ . Thus, structural properties and decay energies are plotted and estimated for prolate shaped throughout the chain. Moreover, some nuclides do not have all three well-defined shape and we obtain only two solutions of the field equations. As the experimental information of these isotopes is not available, so in order to provide some validity to the predictive power of our model and their results a comparison of binding energies of our calculations with those obtained from FRDM [89, 90] is made wherever available and somehow close agreement is found among them. From Table 1, we can see that the binding energies difference between RMF and FRDM is very small. The maximum difference between RMF and FRDM values is about 7 MeV, namely, the relative differences are less than 0.35%. Our calculated one- and two-neutron separation energy also matches well with FRDM estimations. However, there is no agreement in quadrupole deformation parameter within RMF and the values obtained from FRDM data [89, 90]. Some of the nuclides of considered isotopic series, for example  $^{298-318}_{119}$  having large prolate quadrupole deformation parameter and therefore supposed to be superdeformed by their shape. Superdeformation is common phenomenon in RMF calculations, and it plays a significant role for stability of superheavy nuclei. The radii increases with increasing the mass number, and a sudden change in radii indicates the change in shape of the nuclides. In

**Table 1** Binding energy (BE), quadrupole deformation parameter ( $\beta_2$ ) and radii for  $Z = 119$  isotopic chain within three possible shape configurations

Nuclei	BE		$\beta_2$		$r_c$		$r_t$		FRDM		
	prol.	sph.	obl.	sph.	obl.	prol.	sph.	obl.	prol.	sph.	obl.
	prol.	sph.	obl.	prol.	sph.	obl.	prol.	sph.	obl.	prol.	sph.
284 <sub>119</sub>	2004.6	2002.8	0.217	-0.033	6.298	6.238	6.324	6.263	1997.6	0.072	
285 <sub>119</sub>	2012.6	2011.9	0.203	-0.068	6.298	6.248	6.326	6.276	2006.6	0.080	
286 <sub>119</sub>	2020.4	2020.0	0.194	0.045	6.299	6.252	6.332	6.283	2014.5	0.080	
287 <sub>119</sub>	2028.2	2028.4	0.187	0.039	6.301	6.257	6.338	6.292	2023.6	-0.104	
288 <sub>119</sub>	2035.7	2036.7	0.181	0.018	6.304	6.262	6.345	6.301	2031.1	-0.104	
289 <sub>119</sub>	2042.9	2044.9	0.175	-0.002	6.307	6.268	6.352	6.310	2039.5	0.089	
290 <sub>119</sub>	2050.1	2052.9	0.168	-0.001	6.309	6.274	6.358	6.319	2046.9	0.089	
291 <sub>119</sub>	2057.0	2060.6	0.145	-0.001	6.301	6.279	6.355	6.328	2055.2	0.081	
292 <sub>119</sub>	2063.8	2067.8	0.163	-0.001	6.317	6.283	6.375	6.337	2062.2	0.089	
293 <sub>119</sub>	2069.6	2074.6	0.240	-0.001	6.370	6.286	6.424	6.345	2070.4	0.081	
294 <sub>119</sub>	2076.4	2081.1	0.243	-0.001	6.379	6.290	6.436	6.353	2077.2	0.081	
295 <sub>119</sub>	2083.0	2087.6	0.245	-0.002	6.386	6.293	6.446	6.361	2084.7	0.072	
296 <sub>119</sub>	2089.5	2094.0	0.246	-0.001	6.393	6.296	6.457	6.369	2090.9	-0.096	
297 <sub>119</sub>	2096.0	2100.4	0.247	-0.001	6.400	6.299	6.467	6.377	2098.6	-0.079	
298 <sub>119</sub>	2110.2	2106.8	0.555	-0.001	6.609	6.302	6.669	6.385	2105.0	-0.044	
299 <sub>119</sub>	2116.7	2113.1	0.559	-0.001	6.619	6.305	6.683	6.393	2112.0	-0.018	
300 <sub>119</sub>	2122.9	2119.4	0.565	0.000	6.630	6.308	6.697	6.401	2117.8	-0.008	
301 <sub>119</sub>	2129.1	2125.5	0.578	0.000	6.647	6.311	6.718	6.418	2124.3	0.000	
302 <sub>119</sub>	2135.3	2131.5	0.586	0.000	6.661	6.315	6.736	6.418	2129.7	0.000	
303 <sub>119</sub>	2141.2	2137.1	0.588	0.000	6.670	6.320	6.748	6.427	2135.9	0.000	
304 <sub>119</sub>	2147.1	2142.5	0.589	0.000	6.678	6.326	6.758	6.437	2140.3	0.000	
305 <sub>119</sub>	2152.8	2147.6	0.589	0.000	6.685	6.333	6.769	6.448	2146.5	0.000	
306 <sub>119</sub>	2158.3	2152.5	0.592	0.000	6.694	6.342	6.781	6.459	2150.6	0.001	
307 <sub>119</sub>	2163.6	2157.4	0.598	-0.001	6.706	6.351	6.796	6.470	2156.4	0.000	
308 <sub>119</sub>	2168.8	2162.3	0.606	0.012	6.721	6.360	6.813	6.481	2160.6	0.001	
309 <sub>119</sub>	2174.0	2167.4	0.613	0.030	6.734	6.370	6.830	6.493	2166.1	0.001	
310 <sub>119</sub>	2178.9	2172.4	0.619	0.039	6.747	6.380	6.846	6.505	2170.4	0.002	
311 <sub>119</sub>	2183.9	2177.4	0.627	0.043	6.760	6.390	6.863	6.517	2176.0	0.003	
312 <sub>119</sub>	2190.7	2182.4	0.741	0.044	6.882	6.399	6.981	6.528	2180.1	0.004	
313 <sub>119</sub>	2196.0	2187.2	0.743	0.042	6.892	6.408	6.993	6.539	2185.7	0.004	
314 <sub>119</sub>	2197.2	2192.0	0.569	0.035	6.723	6.416	6.838	6.549	2196.3	0.531	

**Table 1** continued

Nuclei	BE		$\beta_2$		$r_c$		$r_t$		FRDM				
	prol.	obl.	prol.	obl.	prol.	obl.	prol.	obl.	BE	$\beta_2$			
315 <sub>119</sub>	2200.6	2196.8	0.458	2197.8	0.000	-0.247	6.637	6.425	6.506	6.757	6.633	2202.0	0.541
316 <sub>119</sub>	2205.6	2201.6	0.450	2202.4	0.000	-0.253	6.638	6.434	6.517	6.761	6.648	2206.4	0.542
317 <sub>119</sub>	2210.3	2206.3	0.445	2207.1	0.000	-0.259	6.640	6.442	6.527	6.768	6.661	2208.5	0.360
318 <sub>119</sub>	2214.9	2210.6	0.429	2211.7	0.000	-0.264	6.634	6.449	6.537	6.767	6.674	2212.5	0.331
319 <sub>119</sub>	2219.3	2214.5	0.386	2216.3	0.000	-0.269	6.606	6.456	6.547	6.746	6.688	2217.9	0.331
320 <sub>119</sub>	2224.0	2218.2	0.373	2220.7	0.000	-0.274	6.603	6.462	6.556	6.747	6.701	2222.0	0.331
321 <sub>119</sub>	2228.6	2221.7	0.360	2225.3	0.001	-0.279	6.600	6.468	6.565	6.748	6.714	2227.0	0.331
322 <sub>119</sub>	2233.2	2229.6	0.336	2229.6	0.000	-0.284	6.589	6.468	6.573	6.739	6.726	2230.9	0.322
323 <sub>119</sub>	2237.7	2231.9	0.328	2231.9	0.000	-0.191	6.591	6.526	6.526	6.744	6.682	2235.6	0.322
324 <sub>119</sub>	2242.2	2236.1	0.320	2236.1	0.000	-0.189	6.592	6.532	6.532	6.749	6.691	2239.1	0.322
325 <sub>119</sub>	2246.7	2240.4	0.313	2240.4	0.000	-0.189	6.594	6.538	6.538	6.755	6.701	2243.5	0.322
326 <sub>119</sub>	2250.9	2244.4	0.307	2244.4	0.000	-0.191	6.596	6.545	6.545	6.761	6.711	2247.0	0.312
327 <sub>119</sub>	2255.1	2248.5	0.300	2248.5	0.000	-0.195	6.597	6.552	6.552	6.766	6.722	2251.3	0.313
328 <sub>119</sub>	2259.2	2252.4	0.292	2252.4	0.000	-0.199	6.596	6.559	6.559	6.770	6.733	2254.7	0.314
329 <sub>119</sub>	2263.3	2256.2	0.283	2256.2	0.000	-0.204	6.596	6.566	6.566	6.774	6.745	2259.0	0.325
330 <sub>119</sub>	2267.4	2260.0	0.275	2260.0	0.000	-0.210	6.596	6.574	6.574	6.779	6.757	2264.1	0.405
331 <sub>119</sub>	2271.4	2267.4	0.269	2267.4	0.000	-0.386	6.597	6.725	6.725	6.785	6.904	2268.3	0.394
332 <sub>119</sub>	2275.4	2271.8	0.267	2271.8	0.000	-0.415	6.602	6.760	6.760	6.793	6.943	2271.4	0.394
333 <sub>119</sub>	2279.2	2275.5	0.267	2275.5	0.000	-0.405	6.607	6.755	6.755	6.803	6.942	2273.5	0.116
334 <sub>119</sub>	2283.0	2279.1	0.268	2279.1	0.000	-0.391	6.613	6.748	6.748	6.813	6.938	2276.7	0.117
335 <sub>119</sub>	2286.7	2282.9	0.268	2282.9	0.000	-0.383	6.619	6.745	6.745	6.823	6.938	2280.7	0.108
336 <sub>119</sub>	2290.5	2286.7	0.269	2286.7	0.000	-0.378	6.625	6.747	6.747	6.832	6.943	2283.8	0.108
337 <sub>119</sub>	2294.1	2290.3	0.269	2290.3	0.000	-0.377	6.630	6.751	6.751	6.842	6.950	2288.0	0.108
338 <sub>119</sub>	2297.8	2293.8	0.268	2293.8	0.000	-0.377	6.636	6.757	6.757	6.851	6.960	2291.0	0.108
339 <sub>119</sub>	2301.3	2297.1	0.265	2297.1	0.000	-0.378	6.641	6.764	6.764	6.860	6.970	2295.0	0.108
340 <sub>119</sub>	2304.8	2294.7	0.261	2294.7	0.000	-0.193	6.647	6.613	6.613	6.868	6.840		
341 <sub>119</sub>	2308.2	2298.0	0.258	2298.0	0.000	-0.188	6.652	6.616	6.616	6.876	6.847		
342 <sub>119</sub>	2311.2	2301.2	0.255	2301.2	0.000	-0.185	6.658	6.620	6.620	6.885	6.854		
343 <sub>119</sub>	2314.2	2304.3	0.253	2304.3	0.000	-0.183	6.663	6.625	6.625	6.894	6.862		
344 <sub>119</sub>	2317.0	2307.4	0.251	2307.4	0.000	-0.180	6.669	6.629	6.629	6.904	6.870		
345 <sub>119</sub>	2319.8	2310.4	0.249	2310.4	0.000	-0.178	6.674	6.634	6.634	6.913	6.878		
346 <sub>119</sub>	2322.6	2313.3	0.247	2313.3	0.000	-0.176	6.679	6.639	6.639	6.922	6.886		

**Table 1** continued

Nuclei	BE		$\beta_2$		$r_c$		$r_t$		FRDM		
	prol.	obl.	prol.	obl.	prol.	obl.	prol.	obl.	BE	$\beta_2$	
	sph.	sph.	sph.	sph.	sph.	sph.	sph.	sph.	sph.	obl.	
347 <sub>119</sub>	2325.3	2316.4	0.245	-0.174	6.683	6.643	6.931	6.894			6.894
348 <sub>119</sub>	2328.0	2319.3	0.243	-0.172	6.687	6.648	6.940	6.902			6.902
349 <sub>119</sub>	2330.7	2322.2	0.241	-0.169	6.691	6.653	6.949	6.910			6.910
350 <sub>119</sub>	2333.4	2325.2	0.239	-0.166	6.695	6.658	6.958	6.918			6.918
351 <sub>119</sub>	2335.9	2328.1	0.237	-0.162	6.699	6.663	6.968	6.926			6.926
352 <sub>119</sub>	2338.0	2331.0	0.234	-0.159	6.704	6.667	6.977	6.934			6.934
353 <sub>119</sub>	2339.7	2333.9	0.228	-0.156	6.708	6.672	6.984	6.942			6.942
354 <sub>119</sub>	2341.6	2336.8	0.221	-0.155	6.711	6.677	6.991	6.951			6.951
355 <sub>119</sub>	2343.4	2339.7	0.214	-0.155	6.714	6.682	6.998	6.960			6.960
356 <sub>119</sub>	2345.3	2342.5	0.207	-0.155	6.717	6.687	7.005	6.969			6.969
357 <sub>119</sub>	2347.2	2345.2	0.194	-0.156	6.720	6.692	7.009	6.979			6.979
358 <sub>119</sub>	2349.2	2347.6	0.187	-0.181	6.723	6.712	7.016	7.001			7.001
359 <sub>119</sub>	2351.1	2350.1	0.181	-0.188	6.725	6.723	7.023	7.015			7.015
360 <sub>119</sub>	2352.9	2352.2	0.176	-0.185	6.725	6.727	7.031	7.023			7.023
361 <sub>119</sub>	2354.8	2354.3	0.171	-0.179	6.726	6.729	7.039	7.030			7.030
362 <sub>119</sub>	2356.8	2356.2	0.166	-0.173	6.728	6.730	7.048	7.036			7.036
363 <sub>119</sub>	2358.6	2358.2	0.161	-0.167	6.730	6.731	7.056	7.043			7.043
364 <sub>119</sub>	2360.3	2360.3	0.153	-0.160	6.730	6.732	7.062	7.050			7.050
365 <sub>119</sub>	2361.8	2362.4	0.143	-0.154	6.729	6.733	7.066	7.057			7.057
366 <sub>119</sub>	2363.1	2364.3	0.162	-0.154	6.743	6.738	7.089	7.067			7.067
367 <sub>119</sub>	2364.3	2366.4	0.168	-0.154	6.752	6.743	7.106	7.077			7.077
368 <sub>119</sub>	2365.7	2368.5	0.177	-0.150	6.772	6.746	7.111	7.086			7.086
369 <sub>119</sub>	2366.2	2370.5	0.195	-0.138	6.793	6.746	7.131	7.092			7.092
370 <sub>119</sub>	2367.7	2372.7	0.203	-0.185	6.806	6.714	7.145	7.122			7.122
371 <sub>119</sub>	2369.1	2374.7	0.206	-0.201	6.815	6.716	7.156	7.140			7.140
372 <sub>119</sub>	2370.2	2376.5	0.209	-0.207	6.824	6.718	7.168	7.154			7.154
373 <sub>119</sub>	2371.3	2378.2	0.215	-0.215	6.834	6.719	7.182	7.169			7.169
374 <sub>119</sub>	2372.4	2379.9	0.224	-0.228	6.842	6.720	7.195	7.187			7.187
375 <sub>119</sub>	2373.5	2381.5	0.236	-0.238	6.849	6.721	7.209	7.204			7.204



**Fig. 1** Binding energy, quadrupole deformation parameter, one- and two-neutron separation energy are given as function of mass number

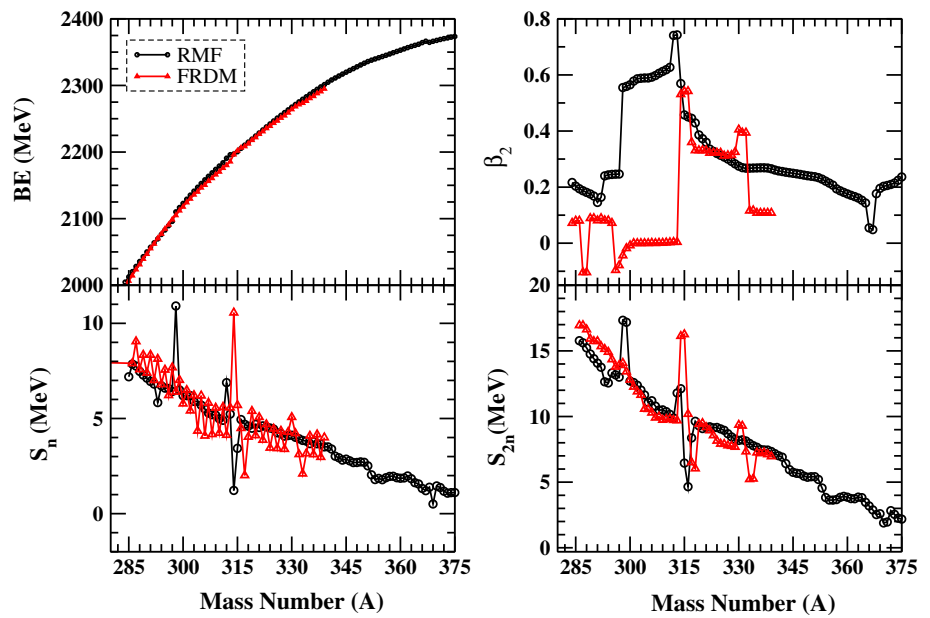
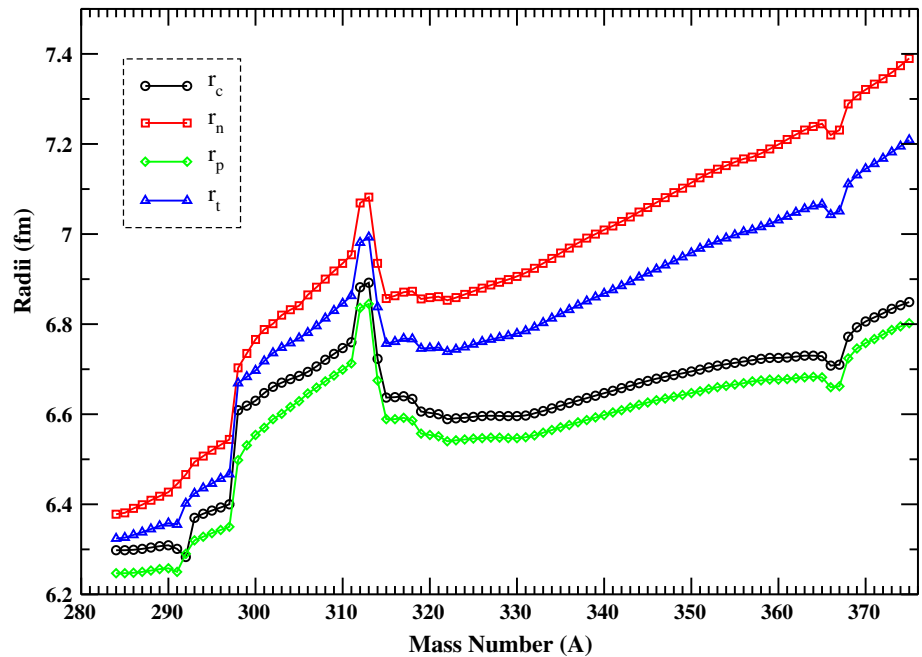


**Fig. 2** Radii as a function of mass number

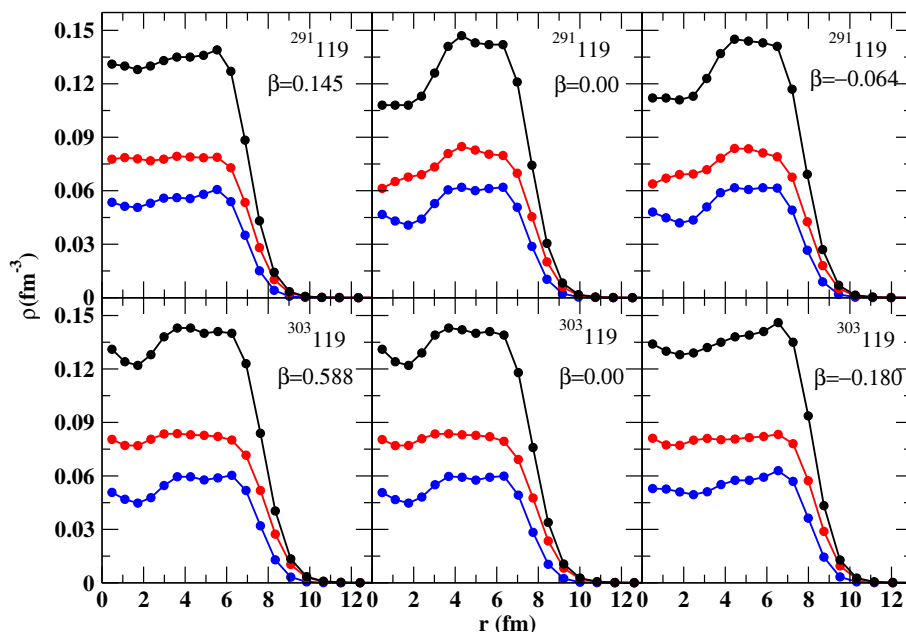


general, the calculated binding and separation energies from RMF are in good agreement with those of the FRDM values wherever available.

### 3.2 Neutron–separation energy

Separation energy is the first prime signature to identify the magic behaviour of the nuclei. The magic numbers in nuclei are characterized by large shell gaps in their single-particle energy levels. Large shell gap means the nucleons occupying the lower energy level have comparatively large value of energy than those nucleons occupying the higher energy levels. This large energy difference between two consecutive energy levels can be observed from the sudden fall of neutron separation energy which attribute the extra stability to a particular nucleus having certain numbers of nucleons and that is why closed shell nuclei are more bound than their nearby ones. Moreover, two-neutron separation energy is more significant than one neutron because it takes care of

**Fig. 3** Total, neutron and proton density distribution as a function of radial parameter for three possible shape configurations. Lines with black, red and blue colours represent the total, neutron and proton density profile, respectively



even-odd staggering and it, therefore, manifests the magicity more clearly. One- and two-neutron separation energy is calculated by the difference in binding energies of two isotopes using the relations

$$S_n(N, Z) = BE(N, Z) - BE(N - 1, Z),$$

$$S_{2n}(N, Z) = BE(N, Z) - BE(N - 2, Z). \quad (18)$$

One- and two-neutron separation energy for the considered isotopic series of the nuclei  $^{284-375}_{119}$  is plotted in lower panel of Fig. 1. No sudden fall of the separation energies is noticed in the present analysis which indicates that as such no neutron magic behaviour within this force parameter is exhibited.

### 3.3 Shape coexistence

The shape of a nucleus is one of the fundamental properties along with its mass and radius. It is the result of the interplay between macroscopic liquid-drop like properties of the nuclear matter and microscopic shell effects. In some areas of the nuclear chart, the shape is seen to be very sensitive to structural effect and may change from one nucleus to its neighbour. These changes are caused by the rearrangement of the orbital configuration of the nucleons or by the dynamic response of the nucleus to rotation. However, there might arise a situation where we may witness that configurations corresponding to different shapes may coexist at similar energies or by a very little difference. The small binding energy difference between two shape configurations makes the structure more complex and the study of such nuclei enrich our understanding of the oscillations of nuclei occurring between two or three existing shapes. This leads isomers can appear in superheavy region. The phenomenon of shape coexistence is ubiquitous as it has been observed throughout the nuclear landscape starting from light nuclei [91] to the regions of heavy nuclei [92, 93] and of course in superheavy region [94–98]. No case of shape coexistence is observed in considered isotopic chain of  $Z = 119$ . However, shape coexistence can be a common phenomenon in superheavy nuclei and thus it is interesting to study it by future experiments. Here, we noticed a very little energy difference around  $\leq 1$  MeV in first and second intrinsic excited states in some of the nuclides. For example, in  $^{298-318}_{119}$  nuclides the excited energy differed by the amount of  $\leq 1$  MeV within spherical and oblate configurations, whereas prolate suggested to be ground state.

### 3.4 Density profile

In general, the neutron excess becomes larger with increasing the mass number and of course it is quite natural in case of superheavy nuclei providing the largest neutron excesses. However, these nuclei also have large number of protons and therefore huge Coulomb repulsion exists there that pushes the proton to larger radii and as a result change the proton density distribution. In this view, neutron and proton density distributions are considered to be great source of potential providing fundamental information on nuclear structure and quite useful to identify the special kinds of features of nuclei such as Bubble, Halo/Skin and cluster structures. Such features are observed in light to superheavy nuclei [99–104]. In the search of such exotic structures, we have made the plot for total, neutron and proton density profile for predicting neutron shell closure nuclei  $^{291}_{119}$  and  $^{303}_{119}$  within this framework as

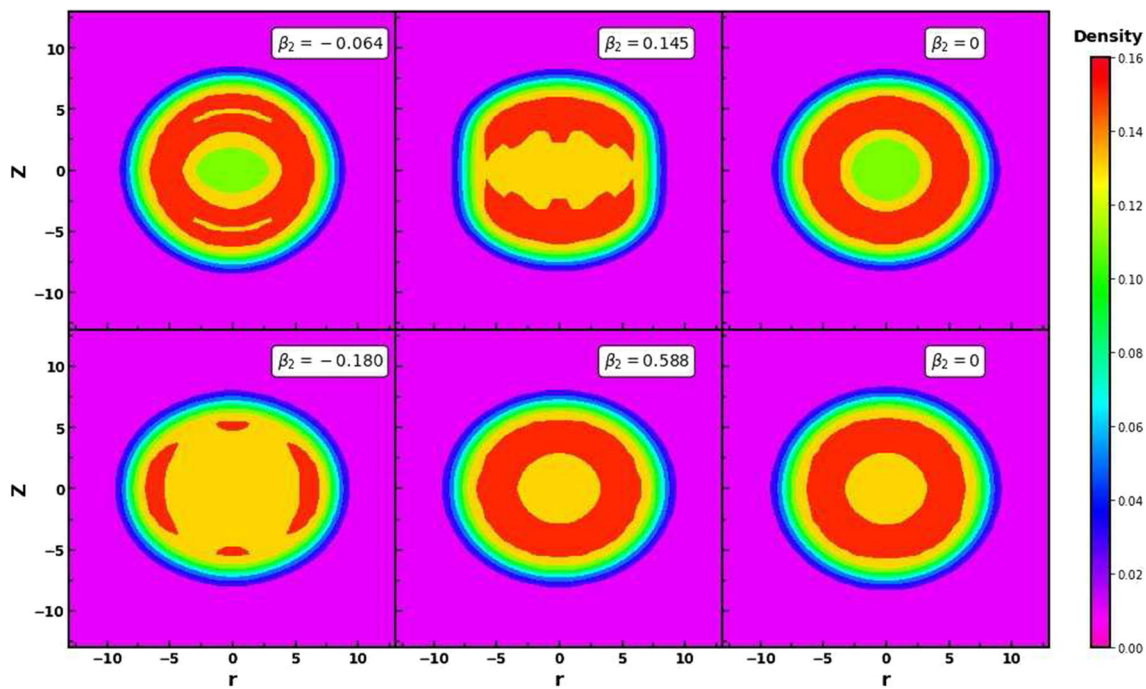


**Fig. 4** Two-dimensional total matter density contours of  $^{291}_{119}$  and  $^{303}_{119}$  for three different shape configurations. Density profile of  $^{291}_{119}$  is seen in upper panel of the figure, while the density distribution of  $^{303}_{119}$  is represented in lower panel

shown in Fig. 3. The spherical configuration of these two nuclides shows the depletion of central part of neutron, proton and total matter (neutron plus proton) density. At prolate configuration the density dies at  $r = 8\text{ fm}$ , while it reaches to  $10\text{ fm}$  in oblate and spherical configurations. This distribution signals prolate as a ground state of these nuclides. Moreover, spherical structure of these two nuclides indicates a special kind of proton distribution, in which the centre is little bulgy and a considerably depletion afterward but again a big hump and further distribution tends to zero at the end of the surface following a decreasing pattern. To reveal such anomalous behaviour of nucleon distribution and to visualize the arrangement of nucleons more clearly inside the nuclei, we make two-dimensional contour plots for  $^{291}_{119}$  and  $^{303}_{119}$  within three different shape configurations as given in Fig. 4. The full red contour refers to maximum density and full pink ones to zero density region. Figure 4 reflects that the hollow region at the centre is spread over the radius of  $1 - 3\text{ fm}$  in spherical configuration. A considerable depopulation is revealed in spherical shape which may supposed to be semi-bubble-type structure. It is also apparent that the region from  $3 - 6\text{ fm}$  of total matter density distribution in both the nuclei is highly dense and formed a thick ring-type structure. It can be interpreted as a somehow hollow central part is surrounded by a thick sheath of nucleons (high density) and formed a thick ring-type structure in prolate shaped. For both the nuclei, in prolate and oblate configurations, the matter distribution is not uniform and bunches of nucleons far from the centre are seen. These bunches may be the cluster of nucleons or alpha particles. Some spindle-type structure is also noticed in prolate configuration having flaps/bulges shapes. In general, cluster, semi-bubble as well as thick ring-type structure is seen.

### 3.5 Decay-energies and half-lives

Superheavy nuclei are identified by  $\alpha$ -decay followed by spontaneous fission as we have mentioned earlier. Decay energy  $Q_\alpha$  is the basic parameter to understand the  $\alpha$ -decay and used to calculate the half-lives. It is observed in alpha-emission and new nucleus is identified. The knowledge of  $Q_\alpha$  of a nucleus gives a valuable information about its stability. Decay energy is estimated by knowing the binding energies of the parent and daughter nuclei and binding energy of  $^4\text{He}$  nucleus. Here, the binding energies are calculated using the most reliable framework of relativistic mean-field model.  $Q_\alpha$  is used as a basic input for calculating the  $\alpha$ -decay half-life. The quantity  $Q_\alpha$  is estimated using the relation

$$Q_\alpha(N, Z) = BE(N - 2, Z - 2) + BE(2, 2) - BE(N, Z). \tag{19}$$

Here,  $BE(N, Z)$ ,  $BE(N - 2, Z - 2)$ , and  $BE(2, 2)$  are the binding energies of the parent, daughter and  $^4\text{He}$  ( $BE = 28.296\text{ MeV}$  [108]) with neutron number  $N$  and proton number  $Z$ . The values of  $Q_\alpha$  for ground state to ground (i.e. prolate) are estimated from RMF binding energy and are given in Tables 2, 3, 4. In order to predict the dominant mode of decay of considered chain, we make the calculations for  $\alpha$ -decay,  $\beta$ -decay and spontaneous fission using various empirical formulas and comparison of their life times shall provide the required results about the mode of decay. The alpha decay half-lives are estimated using various empirical formulas given in the literature such as Viola-Seaborg (VSS) [36], Brown [37], Royer [38], generalized liquid drop model (GLDM) [39], Ni

**Table 2** Decay energies (in MeV) and half-lives of  $\alpha$ ,  $\beta$  and spontaneous fission for  $Z = 119$  isotopic chain and prediction of mode of decays is given

Nuclei	$Q_{\alpha}^{RMF}$	$Q_{\alpha}^{FRDM}$	$\log(T_{1/2}^{\alpha})$				FRDM	Ren-Xu	$Q_{\beta}^{RMF}$	$Q_{\beta}^{FRDM}$	$\log(T_{1/2}^{\beta})$	Fiset-Nix	$T_{1/2}^{\beta}(s)$	Mode of decay
			VSS	Brown	Royer	GLDM								
284 119	14.00	13.02	-6.29	-6.98	-6.86	-6.64	-7.29	-4.42	-6.33	14.29	10.35	0.03	3.73	$\alpha$
285 119	13.89	13.79	-6.43	-6.79	-6.67	-6.81	-7.66	-6.25	-1.77	14.41	8.80	0.05	3.63	$\alpha$
286 119	13.83	13.74	-5.97	-6.69	-6.57	-6.33	-7.00	-5.81	1.95	14.47	9.69	0.03	5.75	$\alpha$
287 119	13.79	13.45	-6.26	-6.63	-6.53	-6.67	-7.51	-5.60	4.84	14.50	7.97	0.05	4.45	$\alpha$
288 119	13.99	13.38	-6.27	-6.95	-6.90	-6.69	-7.26	-5.14	6.90	14.30	8.87	0.03	5.82	$\alpha$
289 119	14.12	13.35	-6.84	-7.15	-7.15	-7.30	-8.01	-5.79	8.15	7.92	7.55	0.22	12.84	$\alpha$
290 119	14.22	13.36	-6.68	-7.31	-7.35	-7.16	-7.61	-5.09	8.59	7.67	8.21	0.06	21.97	$\alpha$
291 119	14.38	13.20	-7.30	-7.56	-7.64	-7.80	-8.40	-5.13	8.24	7.43	6.76	0.38	41.09	$\alpha$
292 119	14.45	13.17	-7.08	-7.66	-7.78	-7.62	-7.95	-4.71	7.10	6.53	7.71	0.45	27.00	$\alpha$
293 119	15.32	12.88	-8.86	-8.92	-9.22	-9.39	-9.73	-4.47	5.17	6.30	6.03	0.78	73.84	$\alpha$
294 119	15.13	12.80	-8.22	-8.66	-8.95	-8.87	-8.93	-3.97	2.47	5.98	6.85	0.66	80.88	$\alpha$
295 119	16.18	12.88	-10.16	-10.06	-10.56	-10.73	-10.85	-4.49	-0.99	4.81	5.45	1.42	>100	$\alpha$
296 119	16.02	13.08	-9.58	-9.86	-10.34	-10.36	-10.10	-4.54	-5.21	5.41	6.77	0.91	28.29	$\alpha$
297 119	16.03	12.74	-9.95	-9.88	-10.38	-10.56	-10.67	-4.19	-10.19	5.10	5.19	1.29	71.00	SF
298 119	11.48	12.50	-1.01	-2.33	-1.84	-1.25	-2.76	-3.34	-15.90	5.01	5.68	1.09	>100	SF
299 119	11.37	12.80	-1.09	-2.10	-1.60	-1.72	-3.09	-4.32	-22.35	3.38	4.18	2.25	>100	SF
300 119	9.96	13.15	3.11	1.28	2.22	3.11	0.76	-4.67	-29.53	9.70	4.92	-0.51	>100	SF
301 119	11.04	13.27	-0.25	-1.30	-0.80	-0.92	-2.37	-5.25	-37.43	4.38	3.55	1.66	>100	SF
302 119	11.09	13.38	-0.04	-1.48	-0.95	-0.29	-1.93	-5.13	-46.04	4.07	4.34	1.58	>100	SF
303 119	11.24	13.38	-0.76	-1.82	-1.34	-1.47	-2.81	-5.46	-55.36	3.72	2.16	2.04	>100	SF
304 119	11.65	14.14	-1.42	-2.70	-2.36	-1.79	-3.11	-6.55	-65.37	3.27	3.99	2.09	>100	SF
305 119	11.95	13.84	-2.47	-3.31	-3.07	-3.21	-4.27	-6.33	-76.08	2.83	1.59	2.66	>100	SF
306 119	6.44	13.97	17.69	14.09	16.65	18.57	13.25	-6.23	-87.48	8.25	3.28	-0.10	>100	SF
307 119	5.88	13.81	20.81	17.12	20.07	20.06	15.65	-6.29	-99.55	8.43	1.27	0.09	>100	SF
308 119	5.31	13.43	25.26	20.73	24.14	26.61	19.72	-5.23	-112.30	1.61	2.64	3.60	>100	SF
309 119	9.03	13.31	5.76	3.91	5.05	4.95	2.77	-3.35	-125.71	1.36	0.96	4.18	>100	SF
310 119	8.88	12.76	6.63	4.38	5.57	6.70	3.78	-3.88	-139.79	1.08	1.99	4.35	>100	SF
311 119	8.91	12.49	6.21	4.30	5.46	5.37	3.16	-3.65	-154.51	0.81	0.51	5.08	>100	SF
312 119	6.81	12.11	15.63	12.27	14.49	16.27	11.48	-2.48	-169.88	1.02	$\pm$	4.46	$\pm$	SF
313 119	6.30	13.25	18.17	14.80	17.34	17.31	13.40	-5.22	-185.90	0.69	6.28	5.33	14.29	SF

**Table 2** continued

Nuclei	$Q_{\alpha}^{RMF}$	$Q_{\alpha}^{FRDM}$	$\log(T_{1/2}^{\alpha})$				FRDM	Ren-Xu	$Q_{\beta}^{RMF}$	$Q_{\beta}^{FRDM}$	$\log(T_{1/2}^{\beta})$	Fiset-Nix	$T_{1/2}^{\beta}(s)$	Mode of decay
			VSS	Brown	Royer	GLDM								
314119	8.28	4.66	8.91	6.37	7.76	9.06	5.73	>20	-202.54	-3.42	1.30	2.00	>100	SF
315119	9.34	4.13	4.70	2.98	3.89	3.79	1.87	>20	-219.82	-4.74	±	1.49	stable	SF
316119	9.17	5.14	5.64	3.50	4.47	5.54	2.93	>20	-237.72	0.45	1.27	5.70	>100	SF
317119	9.25	8.14	5.01	3.25	4.17	4.07	2.14	9.11	-256.23	0.41	3.77	6.04	1.14	SF
318119	9.33	7.84	5.08	3.01	3.88	4.91	2.45	10.74	-275.36	0.05	±	7.47	±	SF
319119	9.40	8.74	4.51	2.81	3.64	3.54	1.71	6.79	-295.09	-0.12	0.57	7.18	>100	SF
320119	9.07	8.68	5.97	3.80	4.74	5.83	3.22	7.36	-315.42	-0.15	2.05	6.77	>100	SF
321119	8.71	8.71	6.91	4.92	5.99	5.90	3.76	6.92	-336.34	-0.34	1.19	6.27	>100	SF
322119	8.42	8.72	8.36	5.90	7.09	8.35	5.26	7.21	-357.85	-0.50	2.69	5.56	>100	SF
323119	8.17	8.98	9.01	6.76	8.05	7.97	5.56	5.94	-379.94	-0.53	1.89	5.72	>100	SF
324119	8.01	9.00	10.00	7.33	8.69	10.06	6.67	6.21	-402.62	-0.70	3.36	5.09	71.06	SF
325119	7.80	8.94	10.57	8.13	9.57	9.50	6.89	6.09	-425.86	-0.88	2.41	4.96	>100	SF
326119	7.87	8.72	10.61	7.87	9.26	10.68	7.18	7.21	-449.67	-1.12	3.73	4.31	22.28	SF
327119	7.82	8.55	10.48	8.05	9.45	9.38	6.82	7.52	-474.04	-1.33	2.82	4.24	17.84	SF
328119	7.80	8.27	10.88	8.11	9.50	10.94	7.42	8.95	-498.97	-1.47	4.08	3.81	31.41	SF
329119	7.72	8.08	10.91	8.43	9.85	9.77	7.18	9.35	-524.45	-1.57	3.16	3.93	54.58	SF
330119	7.53	6.24	12.11	9.19	10.69	12.22	8.47	18.92	-550.47	-1.66	2.57	3.57	>100	SF
331119	7.49	6.03	11.92	9.32	10.82	10.75	8.05	19.87	-577.04	-1.80	1.65	3.66	>100	SF
332119	7.45	5.98	12.48	9.51	11.02	12.58	8.79	>20	-604.14	-2.01	2.96	3.19	>100	SF
333119	7.44	7.82	12.16	9.53	11.03	10.96	8.26	10.48	-631.78	-2.22	5.96	3.22	0.08	SF
334119	7.33	7.57	13.05	10.01	11.56	13.15	9.27	11.9	-659.94	-2.41	4.85	2.80	>100	SF
335119	7.17	7.42	13.46	10.67	12.29	12.23	9.37	12.28	-688.62	-2.60	3.61	2.88	>100	SF
336119	6.91	7.16	15.12	11.83	13.59	15.33	11.05	13.86	-717.83	-2.79	5.02	2.49	4.52	SF
337119	6.72	6.76	15.78	12.70	14.57	14.51	11.35	15.58	-747.54	-2.97	3.86	2.60	43.33	SF
338119	6.53	6.54	17.17	13.62	15.59	17.48	12.80	17.11	-777.76	-3.15	5.33	2.22	9.55	SF
339119	6.39	6.36	17.63	14.33	16.38	16.34	12.94	17.82	-808.49	-3.38	4.32	2.30		SF
340119	6.32		18.44	14.74	16.83	18.81	13.89		-839.72	-3.65		1.89		SF
341119	6.12		19.29	15.79	18.00	17.96	14.35		-871.44	-3.99		1.93		SF
342119	6.09		19.81	15.95	18.17	20.24	15.06		-903.65	-4.46		1.43		SF
343119	6.00		20.05	16.46	18.73	18.70	15.01		-936.35	-4.80		1.50		SF
344119	5.89		21.08	17.06	19.40	21.57	16.15		-969.33	-5.03		1.15		SF

**Table 2** continued

Nuclei	$Q_{\alpha}^{RMF}$	$Q_{\alpha}^{FRDM}$	$\log(T_{1/2}^{\alpha})$		Brown	Royer	GLDM	Ni et al.	FRDM	$\log(T_{1/2}^{SF})$	$Q_{\beta}^{RMF}$	$Q_{\beta}^{FRDM}$	$\log(T_{1/2}^{\beta})$	Fiset-Nix	$T_{1/2}^{\beta}(s)$	Mode of decay
			VSS	FRDM												
<sup>345</sup> 119	5.61		22.72	17.30	18.80	21.36	21.34	17.30		-1003.18	-5.25		1.29		SF	
<sup>346</sup> 119	5.30		25.32	19.78	20.79	23.60	26.07	19.78		-1037.32	-5.49		0.95		SF	
<sup>347</sup> 119	5.16		26.12	20.20	21.79	24.71	24.71	20.20		-1071.92	-5.68		1.11		SF	
<sup>348</sup> 119	4.90		28.66	22.63	23.71	26.88	29.59	22.63		-1106.98	-5.82		0.81		SF	
<sup>349</sup> 119	4.67		30.35	23.82	25.50	28.89	28.91	23.82		-1142.51	-5.93		1.01		SF	
<sup>350</sup> 119	4.48		32.58	25.99	27.16	30.76	33.75	25.99		-1178.50	-6.05		0.72		SF	
<sup>351</sup> 119	4.49		32.13	25.34	27.06	30.63	30.66	25.34		-1214.94	-6.29		0.87		SF	
<sup>352</sup> 119	5.00		27.78	21.88	22.94	25.95	28.59	21.88		-1251.83	-6.88		0.41		SF	
<sup>353</sup> 119	5.65		22.40	17.02	18.52	20.91	20.89	17.02		-1289.16	-7.24		0.53		SF	
<sup>354</sup> 119	5.69		22.46	17.33	18.27	20.62	22.88	17.33		-1326.94	-7.32		0.27		SF	
<sup>355</sup> 119	5.56		23.07	17.60	19.11	21.56	21.53	17.60		-1365.16	-7.37		0.49		SF	
<sup>356</sup> 119	5.38		24.70	19.25	20.24	22.82	25.25	19.25		-1403.81	-7.45		0.23		SF	
<sup>357</sup> 119	5.19		25.84	19.96	21.54	24.28	24.27	19.96		-1442.89	-7.43		0.48		SF	
<sup>358</sup> 119	5.05		27.36	21.52	22.57	25.44	28.05	21.52		-1482.40	-7.48		0.22		SF	
<sup>359</sup> 119	4.86		28.67	22.38	24.02	27.07	27.07	22.38		-1522.34	-7.60		0.42		SF	
<sup>360</sup> 119	4.91		28.58	22.57	23.64	26.62	29.32	22.57		-1562.69	-7.69		0.15		SF	
<sup>361</sup> 119	4.86		28.60	22.32	23.96	26.96	26.97	22.32		-1603.47	-7.71		0.39		SF	
<sup>362</sup> 119	4.67		30.69	24.37	25.50	28.70	31.55	24.37		-1644.65	-7.73		0.14		SF	
<sup>363</sup> 119	4.61		30.97	24.35	26.04	29.30	29.31	24.35		-1686.25	-7.83		0.36		SF	
<sup>364</sup> 119	4.80		29.47	23.33	24.43	27.45	30.22	23.33		-1728.25	-10.22		-0.54		SF	
<sup>365</sup> 119	4.97		27.65	21.51	23.13	25.96	25.96	21.51		-1770.65	-8.13		0.27		SF	
<sup>366</sup> 119	4.11		36.49	29.34	30.59	34.41	37.68	29.34		-1813.46	-6.12		0.72		SF	
<sup>367</sup> 119	3.55		43.17	34.80	36.76	41.39	41.47	34.80		-1856.66	-5.67		1.14		SF	
<sup>368</sup> 119	6.37		18.11	13.60	14.45	16.07	18.03	13.60		-1900.26	-9.08		-0.24		SF	
<sup>369</sup> 119	6.63		16.30	11.79	13.16	14.60	14.53	11.79		-1944.24	-9.16		-0.02		SF	
<sup>370</sup> 119	7.02		14.58	10.59	11.36	12.53	14.24	10.59		-1988.62	-9.28		-0.29		SF	
<sup>371</sup> 119	3.48		44.22	35.69	37.67	42.38	42.46	35.69		-2033.38	-9.41		-0.08		SF	
<sup>372</sup> 119	3.39		45.85	37.35	38.81	43.65	47.58	37.35		-2078.51	-9.66		-0.39		SF	
<sup>373</sup> 119	3.27		47.46	38.46	40.52	45.57	45.67	38.46		-2124.03	-9.92		-0.21		SF	
<sup>374</sup> 119	3.07		51.07	41.81	43.39	48.81	53.12	41.81		-2169.92	-10.15		-0.51		SF	
<sup>375</sup> 119	2.99		52.30	42.61	44.77	50.37	50.49	42.61		-2216.19	-10.18		-0.27		SF	

**Table 3** Same as Table 2 but for the study of  $\alpha$ -decay chains of fission survival nuclides (i.e.  $^{284-296}119$ ) of the considered isotopic chain. Experimental data for  $Q_\alpha$  [105–107], if available, are given in parentheses with asterisk

Nuclei	$Q_\alpha^{RMF}$	$T_{1/2}^\alpha$					$T_{1/2}^{SF}$	Mode of decay
		VSS	Brown	Royer	GLDM	Ni et al.		
$^{284}119$	14.005	$0.502 \times 10^{-06}$	$0.106 \times 10^{-06}$	$0.139 \times 10^{-06}$	$0.227 \times 10^{-06}$	$0.518 \times 10^{-07}$	1.174	$\alpha 1$
$^{280}\text{Ts}$	13.257	$0.398 \times 10^{-05}$	$0.615 \times 10^{-06}$	$0.102 \times 10^{-05}$	$0.183 \times 10^{-05}$	$0.286 \times 10^{-06}$	– 3.328	SF
$^{276}\text{Mc}$	12.353	$0.783 \times 10^{-04}$	$0.836 \times 10^{-05}$	$0.189 \times 10^{-04}$	$0.392 \times 10^{-04}$	$0.347 \times 10^{-05}$	– 6.446	SF
$^{272}\text{Nh}$	12.032	$0.107 \times 10^{-03}$	$0.109 \times 10^{-04}$	$0.245 \times 10^{-04}$	$0.490 \times 10^{-04}$	$0.432 \times 10^{-05}$	– 8.257	SF
$^{268}\text{Rg}$	11.714	$0.144 \times 10^{-03}$	$0.142 \times 10^{-04}$	$0.317 \times 10^{-04}$	$0.611 \times 10^{-04}$	$0.536 \times 10^{-05}$	– 8.839	SF
$^{285}119$	13.891	$0.368 \times 10^{-06}$	$0.160 \times 10^{-06}$	$0.214 \times 10^{-06}$	$0.153 \times 10^{-06}$	$0.219 \times 10^{-07}$	5.732	$\alpha 1$
$^{281}\text{Ts}$	13.396	$0.982 \times 10^{-06}$	$0.358 \times 10^{-06}$	$0.533 \times 10^{-06}$	$0.388 \times 10^{-06}$	$0.475 \times 10^{-07}$	0.977	$\alpha 2$
$^{277}\text{Mc}$	12.286	$0.494 \times 10^{-04}$	$0.112 \times 10^{-04}$	$0.250 \times 10^{-04}$	$0.189 \times 10^{-04}$	$0.129 \times 10^{-05}$	– 2.409	SF
$^{273}\text{Nh}$	11.873	$0.108 \times 10^{-03}$	$0.222 \times 10^{-04}$	$0.519 \times 10^{-04}$	$0.399 \times 10^{-04}$	$0.240 \times 10^{-05}$	– 4.499	SF
$^{269}\text{Rg}$	11.398	$0.335 \times 10^{-03}$	$0.619 \times 10^{-04}$	$0.155 \times 10^{-03}$	$0.122 \times 10^{-03}$	$0.609 \times 10^{-05}$	– 5.373	SF
$^{292}119$	14.450	$0.828 \times 10^{-07}$	$0.217 \times 10^{-07}$	$0.165 \times 10^{-07}$	$0.238 \times 10^{-07}$	$0.111 \times 10^{-07}$	14.595	$\alpha 1$
$^{288}\text{Ts}$	13.081	$0.875 \times 10^{-05}$	$0.124 \times 10^{-05}$	$0.161 \times 10^{-05}$	$0.304 \times 10^{-05}$	$0.561 \times 10^{-06}$	9.454	$\alpha 2$
$^{284}\text{Mc}$	11.552	$0.462 \times 10^{-02}$	$0.317 \times 10^{-03}$	$0.788 \times 10^{-03}$	$0.219 \times 10^{-02}$	$0.114 \times 10^{-03}$	5.638	$\alpha 3$
$^{280}\text{Nh}$	10.486	$0.510 \times 10^{-00}$	$0.218 \times 10^{-01}$	$0.823 \times 10^{-01}$	$0.302 \times 10^{-00}$	$0.614 \times 10^{-02}$	3.073	$\alpha 4$
$^{276}\text{Rg}$	10.434	$0.166 \times 10^{-00}$	$0.836 \times 10^{-02}$	$0.259 \times 10^{-01}$	$0.827 \times 10^{-01}$	$0.227 \times 10^{-02}$	1.679	$\alpha 5$
$^{272}\text{Mt}$	10.560	$1.890 \times 10^{-02}$	$1.220 \times 10^{-03}$	$2.860 \times 10^{-03}$	$7.360 \times 10^{-03}$	$3.410 \times 10^{-04}$	1.374	$\alpha 6$
$^{268}\text{Bh}$	8.804	$4.150 \times 10^{+02}$	$1.260 \times 10^{+01}$	$6.180 \times 10^{+01}$	$3.070 \times 10^{+02}$	$1.780 \times 10^{+00}$	2.067	SF
$^{264}\text{Db}$	7.442	$6.400 \times 10^{+06}$	$1.110 \times 10^{+05}$	$9.640 \times 10^{+05}$	$9.010 \times 10^{+06}$	$6.990 \times 10^{+03}$	3.665	SF
$^{260}\text{Lr}$	7.144	$1.670 \times 10^{+07}$	$3.450 \times 10^{+05}$	$2.550 \times 10^{+06}$	$2.410 \times 10^{+07}$	$1.600 \times 10^{+04}$	6.069	SF
$^{293}119$	15.317	$0.139 \times 10^{-08}$	$0.120 \times 10^{-08}$	$0.596 \times 10^{-09}$	$0.409 \times 10^{-09}$	$0.185 \times 10^{-09}$	12.670	$\alpha 1$
$^{289}\text{Ts}$	12.984	$0.619 \times 10^{-05}$	$0.183 \times 10^{-05}$	$0.240 \times 10^{-05}$	$0.174 \times 10^{-05}$	$0.230 \times 10^{-06}$	7.668	$\alpha 2$
$^{285}\text{Mc}$	11.603	$0.160 \times 10^{-02}$	$0.248 \times 10^{-03}$	$0.577 \times 10^{-03}$	$0.439 \times 10^{-03}$	$0.254 \times 10^{-04}$	3.990	$\alpha 3$
$^{281}\text{Nh}$	10.317	$0.656 \times 10^{+00}$	$0.556 \times 10^{-01}$	$0.223 \times 10^{+00}$	$0.178 \times 10^{+00}$	$0.421 \times 10^{-02}$	1.563	$\alpha 4$
$^{277}\text{Rg}$	10.169	$0.384 \times 10^{+00}$	$0.363 \times 10^{-01}$	$0.126 \times 10^{+00}$	$0.102 \times 10^{+00}$	$0.256 \times 10^{-02}$	0.308	$\alpha 5$
$^{273}\text{Mt}$	10.508	$1.160 \times 10^{-02}$	$1.610 \times 10^{-03}$	$3.710 \times 10^{-03}$	$2.990 \times 10^{-03}$	$1.240 \times 10^{-04}$	0.140	$\alpha 6$
$^{269}\text{Bh}$	8.814	$1.750 \times 10^{-02}$	$1.180 \times 10^{+01}$	$5.500 \times 10^{+01}$	$4.740 \times 10^{-01}$	$4.690 \times 10^{-01}$	0.971	$\alpha 7/\text{SF}$
$^{261}\text{Db}$	6.833	$1.780 \times 10^{+08}$	$6.580 \times 10^{+06}$	$5.780 \times 10^{+07}$	$5.530 \times 10^{+07}$	$6.780 \times 10^{+04}$	5.253	SF
$^{294}119$	15.131	$0.607 \times 10^{-08}$	$0.218 \times 10^{-08}$	$0.113 \times 10^{-08}$	$0.135 \times 10^{-08}$	$0.118 \times 10^{-08}$	9.971	$\alpha 1$
$^{290}\text{Ts}$	12.956	$0.155 \times 10^{-04}$	$0.204 \times 10^{-05}$	$0.261 \times 10^{-05}$	$0.514 \times 10^{-05}$	$0.914 \times 10^{-06}$	5.156	$\alpha 2$
$^{286}\text{Mc}$	11.561	$0.440 \times 10^{-02}$	$0.303 \times 10^{-03}$	$0.692 \times 10^{-03}$	$0.192 \times 10^{-02}$	$0.110 \times 10^{-03}$	1.666	$\alpha 3$
$^{282}\text{Nh}$	10.188	$0.325 \times 10^{+01}$	$0.115 \times 10^{+00}$	$0.481 \times 10^{+00}$	$0.201 \times 10^{+01}$	$0.300 \times 10^{-01}$	– 0.573	SF
$^{278}\text{Rg}$	9.925	$0.398 \times 10^{+01}$	$0.148 \times 10^{+00}$	$0.570 \times 10^{+00}$	$0.228 \times 10^{+01}$	$0.345 \times 10^{-01}$	1.639	SF
$^{295}119$	16.177	$0.695 \times 10^{-10}$	$0.868 \times 10^{-10}$	$0.277 \times 10^{-10}$	$0.187 \times 10^{-10}$	$0.142 \times 10^{-10}$	6.507	$\alpha 1$
$^{291}\text{Ts}$	11.763	$0.253 \times 10^{-02}$	$0.372 \times 10^{-03}$	$0.884 \times 10^{-03}$	$0.663 \times 10^{-03}$	$0.396 \times 10^{-04}$	1.925	$\alpha 2$
$^{287}\text{Mc}$	11.332 (10.74)*	$0.695 \times 10^{-02}$	$0.918 \times 10^{-03}$	$0.229 \times 10^{-02}$	$0.176 \times 10^{-02}$	$0.892 \times 10^{-04}$	– 1.329	SF
$^{283}\text{Nh}$	10.097 (10.26)*	$0.581 \times 10^{+01}$	$0.194 \times 10^{+00}$	$0.859 \times 10^{+00}$	$0.375 \times 10^{+01}$	$0.494 \times 10^{-01}$	– 3.443	SF
$^{279}\text{Rg}$	9.666 (10.52)*	$0.221 \times 10^{+02}$	$0.697 \times 10^{+00}$	$0.315 \times 10^{+01}$	$0.143 \times 10^{+02}$	$0.150 \times 10^{+00}$	– 4.273	SF
$^{296}119$	16.017	$0.262 \times 10^{-09}$	$0.139 \times 10^{-09}$	$0.455 \times 10^{-10}$	$0.435 \times 10^{-10}$	$0.803 \times 10^{-10}$	2.285	$\alpha 1$
$^{292}\text{Ts}$	11.596	$0.136 \times 10^{-01}$	$0.822 \times 10^{-03}$	$0.207 \times 10^{-02}$	$0.662 \times 10^{-02}$	$0.304 \times 10^{-03}$	– 2.016	SF
$^{288}\text{Mc}$	11.262 (10.46)*	$0.225 \times 10^{-01}$	$0.130 \times 10^{-02}$	$0.324 \times 10^{-02}$	$0.101 \times 10^{-01}$	$0.443 \times 10^{-03}$	– 4.987	SF
$^{284}\text{Nh}$	9.920 (10.00)*	$0.184 \times 10^{+02}$	$0.547 \times 10^{+00}$	$0.250 \times 10^{+01}$	$0.119 \times 10^{+02}$	$0.133 \times 10^{+00}$	– 6.701	SF
$^{280}\text{Rg}$	9.454 (9.75)*	$0.943 \times 10^{+02}$	$0.260 \times 10^{+01}$	$0.124 \times 10^{+02}$	$0.622 \times 10^{+02}$	$0.521 \times 10^{+00}$	– 7.235	SF

**Table 4** Same as Table 2 but for the study of  $\alpha$ -decay chains of fission survival nuclides (i.e.  $^{284-296}119$ ) of the considered isotopic chain. Experimental data for  $Q_\alpha$  [105–107], if available, are given in parentheses with asterisk

Nuclei	$Q_\alpha^{RMF}$	$T_{1/2}^\alpha$					$T_{1/2}^{SF}$	Mode of decay
		VSS	Brown	Royer	GLDM	Ni et al.		
$^{286}119$	13.827	$0.106 \times 10^{-05}$	$0.203 \times 10^{-06}$	$0.269 \times 10^{-06}$	$0.464 \times 10^{-06}$	$0.981 \times 10^{-07}$	9.451	$\alpha 1$
$^{282}\text{Ts}$	13.296	$0.335 \times 10^{-05}$	$0.528 \times 10^{-06}$	$0.792 \times 10^{-06}$	$0.140 \times 10^{-05}$	$0.246 \times 10^{-06}$	4.491	$\alpha 2$
$^{278}\text{Mc}$	12.306	$0.984 \times 10^{-04}$	$0.103 \times 10^{-04}$	$0.218 \times 10^{-04}$	$0.460 \times 10^{-04}$	$0.422 \times 10^{-05}$	0.891	$\alpha 3$
$^{274}\text{Nh}$	11.668	$0.674 \times 10^{-03}$	$0.568 \times 10^{-04}$	$0.142 \times 10^{-03}$	$0.323 \times 10^{-03}$	$0.209 \times 10^{-04}$	- 1.424	SF
$^{270}\text{Rg}$	11.262	$0.152 \times 10^{-02}$	$0.119 \times 10^{-03}$	$0.305 \times 10^{-03}$	$0.695 \times 10^{-03}$	$0.403 \times 10^{-04}$	- 2.535	SF
$^{287}119$	13.795	$0.553 \times 10^{-06}$	$0.229 \times 10^{-06}$	$0.295 \times 10^{-06}$	$0.210 \times 10^{-06}$	$0.310 \times 10^{-07}$	12.337	$\alpha 1$
$^{283}\text{Ts}$	13.092	$0.379 \times 10^{-05}$	$0.118 \times 10^{-05}$	$0.188 \times 10^{-05}$	$0.138 \times 10^{-05}$	$0.151 \times 10^{-06}$	7.224	$\alpha 2$
$^{279}\text{Mc}$	12.296	$0.470 \times 10^{-04}$	$0.107 \times 10^{-04}$	$0.219 \times 10^{-04}$	$0.165 \times 10^{-04}$	$0.124 \times 10^{-05}$	3.462	$\alpha 3$
$^{275}\text{Nh}$	11.629	$0.376 \times 10^{-03}$	$0.681 \times 10^{-04}$	$0.167 \times 10^{-03}$	$0.128 \times 10^{-03}$	$0.699 \times 10^{-05}$	0.974	$\alpha 4$
$^{271}\text{Rg}$	11.077	$0.188 \times 10^{-02}$	$0.295 \times 10^{-03}$	$0.797 \times 10^{-03}$	$0.631 \times 10^{-03}$	$0.268 \times 10^{-04}$	- 0.318	SF
$^{288}119$	13.939	$0.537 \times 10^{-06}$	$0.112 \times 10^{-06}$	$0.126 \times 10^{-06}$	$0.207 \times 10^{-06}$	$0.548 \times 10^{-07}$	14.401	$\alpha 1$
$^{284}\text{Ts}$	12.970	$0.145 \times 10^{-04}$	$0.193 \times 10^{-05}$	$0.314 \times 10^{-05}$	$0.615 \times 10^{-05}$	$0.865 \times 10^{-06}$	9.184	$\alpha 2$
$^{280}\text{Mc}$	12.042	$0.363 \times 10^{-03}$	$0.328 \times 10^{-04}$	$0.737 \times 10^{-04}$	$0.171 \times 10^{-03}$	$0.129 \times 10^{-04}$	5.310	$\alpha 3$
$^{276}\text{Nh}$	11.541	$0.131 \times 10^{-02}$	$0.103 \times 10^{-03}$	$0.252 \times 10^{-03}$	$0.604 \times 10^{-03}$	$0.370 \times 10^{-04}$	2.703	$\alpha 4$
$^{272}\text{Rg}$	10.971	$0.744 \times 10^{-02}$	$0.502 \times 10^{-03}$	$0.137 \times 10^{-02}$	$0.351 \times 10^{-02}$	$0.158 \times 10^{-03}$	1.284	$\alpha 5$
$^{268}\text{Mt}$	10.409	$4.580 \times 10^{-02}$	$2.730 \times 10^{-03}$	$8.190 \times 10^{-03}$	$2.240 \times 10^{-02}$	$7.280 \times 10^{-04}$	0.967	$\alpha 6$
$^{264}\text{Bh}$	9.358	$8.010 \times 10^{+00}$	$3.350 \times 10^{-01}$	$1.410 \times 10^{+00}$	$5.260 \times 10^{+00}$	$6.000 \times 10^{-02}$	1.665	$\alpha 7/\text{SF}$
$^{260}\text{Db}$	8.543	$5.630 \times 10^{+02}$	$1.930 \times 10^{+01}$	$9.860 \times 10^{+01}$	$4.720 \times 10^{+02}$	$2.290 \times 10^{+00}$	3.282	SF
$^{256}\text{Lr}$	7.690	$1.050 \times 10^{+05}$	$3.020 \times 10^{+03}$	$1.880 \times 10^{+04}$	$1.230 \times 10^{+05}$	$2.060 \times 10^{+02}$	5.718	SF
$^{289}119$	14.116	$0.145 \times 10^{-06}$	$0.706 \times 10^{-07}$	$0.714 \times 10^{-07}$	$0.504 \times 10^{-07}$	$0.982 \times 10^{-08}$	15.650	$\alpha 1$
$^{285}\text{Ts}$	13.015	$0.537 \times 10^{-05}$	$0.161 \times 10^{-05}$	$0.246 \times 10^{-05}$	$0.179 \times 10^{-05}$	$0.205 \times 10^{-06}$	10.379	$\alpha 2$
$^{281}\text{Mc}$	11.770	$0.665 \times 10^{-03}$	$0.114 \times 10^{-03}$	$0.283 \times 10^{-03}$	$0.216 \times 10^{-03}$	$0.119 \times 10^{-04}$	6.445	$\alpha 3$
$^{277}\text{Nh}$	11.462	$0.904 \times 10^{-03}$	$0.149 \times 10^{-03}$	$0.367 \times 10^{-03}$	$0.284 \times 10^{-03}$	$0.149 \times 10^{-04}$	3.770	$\alpha 4$
$^{273}\text{Rg}$	10.931	$0.423 \times 10^{-02}$	$0.615 \times 10^{-03}$	$0.165 \times 10^{-02}$	$0.131 \times 10^{-02}$	$0.537 \times 10^{-04}$	2.278	$\alpha 5$
$^{269}\text{Mt}$	10.211	$6.840 \times 10^{-02}$	$8.070 \times 10^{-03}$	$2.580 \times 10^{-02}$	$2.110 \times 10^{-02}$	$5.670 \times 10^{-04}$	1.882	$\alpha 6$
$^{265}\text{Bh}$	9.216	$9.690 \times 10^{+00}$	$8.220 \times 10^{-01}$	$3.590 \times 10^{+00}$	$3.060 \times 10^{+00}$	$3.900 \times 10^{-02}$	2.494	$\alpha 7/\text{SF}$
$^{261}\text{Db}$	8.316	$1.510 \times 10^{+03}$	$9.990 \times 10^{+01}$	$5.580 \times 10^{+02}$	$4.970 \times 10^{+02}$	$2.950 \times 10^{+00}$	4.019	SF
$^{257}\text{Lr}$	7.597	$1.090 \times 10^{+05}$	$6.530 \times 10^{+03}$	$4.120 \times 10^{+04}$	$3.800 \times 10^{+04}$	$1.180 \times 10^{+02}$	6.356	SF
$^{290}119$	14.219	$0.208 \times 10^{-06}$	$0.487 \times 10^{-07}$	$0.451 \times 10^{-07}$	$0.693 \times 10^{-07}$	$0.244 \times 10^{-07}$	16.093	$\alpha 1$
$^{286}\text{Ts}$	13.114	$0.754 \times 10^{-05}$	$0.108 \times 10^{-05}$	$0.151 \times 10^{-05}$	$0.281 \times 10^{-05}$	$0.494 \times 10^{-06}$	10.817	$\alpha 2$
$^{282}\text{Mc}$	11.617	$0.327 \times 10^{-02}$	$0.232 \times 10^{-03}$	$0.606 \times 10^{-03}$	$0.165 \times 10^{-02}$	$0.848 \times 10^{-04}$	6.872	$\alpha 3$
$^{278}\text{Nh}$	11.057 (11.60)*	$0.182 \times 10^{-01}$	$0.109 \times 10^{-02}$	$0.321 \times 10^{-02}$	$0.926 \times 10^{-02}$	$0.352 \times 10^{-03}$	4.183	$\alpha 4$
$^{274}\text{Rg}$	10.975 (11.15)*	$0.727 \times 10^{-02}$	$0.492 \times 10^{-03}$	$0.124 \times 10^{-02}$	$0.315 \times 10^{-02}$	$0.155 \times 10^{-03}$	2.671	$\alpha 5$
$^{270}\text{Mt}$	10.282 (10.03)*	$9.780 \times 10^{-02}$	$5.450 \times 10^{-03}$	$1.610 \times 10^{-02}$	$4.650 \times 10^{-02}$	$1.400 \times 10^{-03}$	2.250	$\alpha 6$
$^{266}\text{Bh}$	8.901	$2.020 \times 10^{+02}$	$6.530 \times 10^{+00}$	$3.280 \times 10^{+01}$	$1.540 \times 10^{+02}$	$9.610 \times 10^{-01}$	2.833	$\alpha 7/\text{SF}$
$^{262}\text{Db}$	8.132	$1.470 \times 10^{+04}$	$3.980 \times 10^{+02}$	$2.380 \times 10^{+03}$	$1.440 \times 10^{+04}$	$3.780 \times 10^{+01}$	4.325	SF
$^{258}\text{Lr}$	7.446	$9.470 \times 10^{+05}$	$2.350 \times 10^{+04}$	$1.560 \times 10^{+05}$	$1.200 \times 10^{+06}$	$1.360 \times 10^{+03}$	6.625	SF
$^{291}119$	14.378	$0.499 \times 10^{-07}$	$0.278 \times 10^{-07}$	$0.228 \times 10^{-07}$	$0.160 \times 10^{-07}$	$0.396 \times 10^{-08}$	15.739	$\alpha 1$
$^{287}\text{Ts}$	13.071	$0.417 \times 10^{-05}$	$0.129 \times 10^{-05}$	$0.175 \times 10^{-05}$	$0.128 \times 10^{-05}$	$0.164 \times 10^{-06}$	10.506	$\alpha 2$
$^{283}\text{Mc}$	11.570	$0.419 \times 10^{-02}$	$0.291 \times 10^{-03}$	$0.778 \times 10^{-03}$	$0.215 \times 10^{-02}$	$0.105 \times 10^{-03}$	6.523	$\alpha 3$
$^{279}\text{Nh}$	10.712	$0.132 \times 10^{+00}$	$0.649 \times 10^{-02}$	$0.232 \times 10^{-01}$	$0.773 \times 10^{-01}$	$0.193 \times 10^{-02}$	3.859	$\alpha 4$
$^{275}\text{Rg}$	10.962	$0.782 \times 10^{-02}$	$0.525 \times 10^{-03}$	$0.133 \times 10^{-02}$	$0.340 \times 10^{-02}$	$0.165 \times 10^{-03}$	2.374	$\alpha 5$



**Table 4** continued

Nuclei	$Q_{\alpha}^{RMF}$	$T_{1/2}^{\alpha}$					$T_{1/2}^{SF}$	Mode of decay
		VSS	Brown	Royer	GLDM	Ni et al.		
$^{271}\text{Mt}$	10.320	$3.540 \times 10^{-02}$	$4.430 \times 10^{-03}$	$1.230 \times 10^{-02}$	$9.970 \times 10^{-03}$	$3.220 \times 10^{-04}$	2.079	$\alpha 6$
$^{267}\text{Bh}$	8.729	$3.320 \times 10^{+02}$	$2.120 \times 10^{+01}$	$1.130 \times 10^{+02}$	$9.810 \times 10^{+01}$	$8.110 \times 10^{-01}$	2.689	SF
$^{263}\text{Db}$	7.786	$1.270 \times 10^{+05}$	$6.110 \times 10^{+03}$	$4.370 \times 10^{+04}$	$3.970 \times 10^{+04}$	$1.330 \times 10^{+02}$	4.206	SF
$^{259}\text{Lr}$	7.334	$1.220 \times 10^{+06}$	$6.250 \times 10^{+04}$	$4.260 \times 10^{+05}$	$3.980 \times 10^{+05}$	$9.370 \times 10^{+02}$	6.528	SF

et al. [40]. Spontaneous fission half-lives are computed using the semi-empirical formula of Ren and Xu [58]. Here, Fiset and Nix [109] empirical formula is used to calculate the  $\beta$ -decay half-lives.

### 3.5.1 Alpha decay

With the even-even values available at hand, the  $\alpha$ -decay half-life of the isotopic chain under study is estimated by Viola-Seaborg semi-empirical relation

$$\log_{10} T_{1/2}^{\alpha} = \frac{aZ - b}{\sqrt{Q_{\alpha}}} - (cZ + d) + h_{\log}. \tag{20}$$

The values of the parameters  $a, b, c$  and  $d$  are taken from the recent modified parameterizations of Sobiczewski et al [44], which are  $a = 1.66175, b = 8.5166, c = 0.20, d = 33.9069$ . The  $h_{\log}$  is the hindrance factor which takes the care of odd numbers of proton and neutron as given by Viola and Seaborg

$$h_{\log} = \begin{cases} 0.000 & \text{even - even;} \\ 0.772 & \text{odd - even;} \\ 1.066 & \text{even - odd;} \\ 1.114 & \text{odd - odd.} \end{cases} \tag{21}$$

There are also several other phenomenological formulas available in the literature by which the  $\alpha$ -decay half-lives is calculated. The semi-empirical formula proposed by Brown [37] for determining the half-life of superheavy nuclei is given by

$$\log_{10} T_{1/2}^{\alpha} = 9.54(Z - 2)^{0.6} / \sqrt{Q_{\alpha}} - 51.37, \tag{22}$$

where  $Z$ , the atomic number of parent nucleus, and  $Q_{\alpha}$  decay energy are only the input for this formula. Moreover, another theoretical predictions for half-life for heavy and superheavy nuclei by employing a fitting procedure to a set of 373 alpha emitters were developed by Royer [38] with an RMS deviation of 0.42, given as

$$\log_{10} T_{1/2}^{\alpha} = -26.06 - 1.114A^{1/6}\sqrt{Z} + \frac{1.5837Z}{\sqrt{Q_{\alpha}}}, \tag{23}$$

where  $A$  and  $Z$  represent the mass number and charge number of the parent nuclei and  $Q_{\alpha}$  represents the energy released during the reaction. Assuming a similar dependence on  $A, Z$  and  $Q_{\alpha}$ , the above equation was reformulated for a subset of 131 even-even nuclei and a relation was obtained with a RMS deviation of only 0.285, given as

$$\log_{10} T_{1/2}^{\alpha} = -25.31 - 1.1629A^{1/6}\sqrt{Z} + \frac{1.5864Z}{\sqrt{Q_{\alpha}}}. \tag{24}$$

For a subset of 106 even-odd nuclei, the relation given by was further modified with an RMS deviation of 0.39 and is given as,

$$\log_{10} T_{1/2}^{\alpha} = -26.65 - 1.0859A^{1/6}\sqrt{Z} + \frac{1.5848Z}{\sqrt{Q_{\alpha}}}. \tag{25}$$

A similar reformulation was performed for the equation for a subset of 86 odd-even nuclei and 50 odd-odd nuclei. Another formula for  $\alpha$ -decay half-lives based on generalized liquid drop model proposed by Dasgupta-Schubert and Reyes [39] is obtained by fitting the experimental half-lives for 373 alpha emitters, given as

$$\log_{10} T_{1/2}^{\alpha} = a + bA^{1/6}Z^{1/2} + cZ/Q_{\alpha}^{1/2}. \tag{26}$$

The parameters  $a, b$  and  $c$  are given by

**Table 5** CPPM study of  $\alpha$ -decay chains of fission survival nuclides (i.e.  $^{284-290}119$ ). Experimental data for  $Q_\alpha$  [105–107], if available, are given in parentheses with asterisk

Nuclei	$Q_\alpha^{RMF}$	$T_{1/2}^\alpha$		$T_{1/2}^{SF}$	Mode of decay
		CPPM ( RMF $Q_\alpha$ )	CPPM (expt. $Q_\alpha$ )		
$^{284}119$	14.005	$1.17 \times 10^{-07}$		$8.47 \times 10^6$	$\alpha$
$^{280}\text{Ts}$	13.257	$1.05 \times 10^{-06}$		$9.61 \times 10^2$	$\alpha$
$^{276}\text{Mc}$	12.353	$2.49 \times 10^{-05}$		$3.96 \times 10^{-1}$	$\alpha$
$^{272}\text{Nh}$	12.032	$3.29 \times 10^{-05}$		$3.99 \times 10^{-3}$	$\alpha$
$^{268}\text{Rg}$	11.714	$4.33 \times 10^{-05}$		$3.31 \times 10^{-4}$	$\alpha$
$^{285}119$	13.891	$1.94 \times 10^{-07}$		$6.27 \times 10^7$	$\alpha$
$^{281}\text{Ts}$	13.396	$5.20 \times 10^{-07}$		$2.30 \times 10^{04}$	$\alpha$
$^{277}\text{Mc}$	12.286	$3.39 \times 10^{-05}$		$5.12 \times 10^{00}$	$\alpha$
$^{273}\text{Nh}$	11.873	$7.44 \times 10^{-05}$		$6.11 \times 10^{-02}$	$\alpha$
$^{269}\text{Rg}$	11.398	$2.43 \times 10^{-04}$		$4.58 \times 10^{-03}$	$\alpha$

**Table 6** CPPM study of  $\alpha$ -decay chains of fission survival nuclides (i.e.  $^{284-290}119$ ). Experimental data for  $Q_\alpha$  [105–107], if available, are given in parentheses with asterisk

Nuclei	$Q_\alpha^{RMF}$	$T_{1/2}^\alpha$		$T_{1/2}^{SF}$	Mode of decay
		CPPM ( RMF $Q_\alpha$ )	CPPM (expt. $Q_\alpha$ )		
$^{286}119$	13.827	$2.45 \times 10^{-07}$		$7.40 \times 10^{+08}$	$\alpha$
$^{282}\text{Ts}$	13.296	$8.02 \times 10^{-07}$		$2.15 \times 10^{+05}$	$\alpha$
$^{278}\text{Mc}$	12.306	$2.93 \times 10^{-05}$		$1.22 \times 10^{+02}$	$\alpha$
$^{274}\text{Nh}$	11.668	$2.22 \times 10^{-04}$		$1.11 \times 10^{+00}$	$\alpha$
$^{270}\text{Rg}$	11.262	$5.08 \times 10^{-04}$		$9.90 \times 10^{-02}$	$\alpha$
$^{287}119$	13.795	$2.82 \times 10^{-07}$		$5.81 \times 10^{+09}$	$\alpha$
$^{283}\text{Ts}$	13.092	$2.07 \times 10^{-06}$		$1.09 \times 10^{+06}$	$\alpha$
$^{279}\text{Mc}$	12.296	$2.99 \times 10^{-05}$		$1.89 \times 10^{+03}$	$\alpha$
$^{275}\text{Nh}$	11.629	$2.65 \times 10^{-04}$		$8.04 \times 10^{+00}$	$\alpha$
$^{271}\text{Rg}$	11.077	$1.44 \times 10^{-03}$		$7.66 \times 10^{-01}$	$\alpha$
$^{288}119$	13.939	$1.36 \times 10^{-07}$		$2.02 \times 10^{+10}$	$\alpha$
$^{284}\text{Ts}$	12.97	$3.62 \times 10^{-06}$		$8.06 \times 10^{+06}$	$\alpha$
$^{280}\text{Mc}$	12.042	$1.11 \times 10^{-04}$		$1.06 \times 10^{+04}$	$\alpha$
$^{276}\text{Nh}$	11.541	$4.18 \times 10^{-04}$		$5.60 \times 10^{+01}$	$\alpha$
$^{272}\text{Rg}$	10.971	$2.61 \times 10^{-03}$		$7.50 \times 10^{+00}$	$\alpha$
$^{268}\text{Mt}$	10.409	$1.80 \times 10^{-02}$		$2.80 \times 10^{+00}$	$\alpha$
$^{264}\text{Bh}$	9.358	4.59852		$2.80 \times 10^{+00}$	SF
$^{260}\text{Db}$	8.543	443.74		$2.30 \times 10^{+01}$	SF
$^{256}\text{Lr}$	7.69	123998.0		$1.99 \times 10^{+03}$	SF
$^{289}119$	14.116	$5.83 \times 10^{-08}$		$4.81 \times 10^{+10}$	$\alpha$
$^{285}\text{Ts}$	13.015	$2.78 \times 10^{-06}$		$2.27 \times 10^{+07}$	$\alpha$
$^{281}\text{Mc}$	11.77	$4.78 \times 10^{-04}$		$2.76 \times 10^{+04}$	$\alpha$
$^{277}\text{Nh}$	11.462	$6.33 \times 10^{-04}$		$9.11 \times 10^{+01}$	$\alpha$
$^{273}\text{Rg}$	10.931	$3.20 \times 10^{-03}$		$2.90 \times 10^{+01}$	$\alpha$
$^{269}\text{Mt}$	10.211	$6.23 \times 10^{-02}$		$1.04 \times 10^{+01}$	$\alpha$
$^{265}\text{Bh}$	9.216	12.6775		$7.14 \times 10^{+00}$	SF
$^{261}\text{Db}$	8.316	2874.07		$3.47 \times 10^{+01}$	SF
$^{257}\text{Lr}$	7.597	289343.0		$2.89 \times 10^{+03}$	SF
$^{290}119$	14.219	$3.60 \times 10^{-08}$		$1.88 \times 10^{11}$	$\alpha$
$^{286}\text{Ts}$	13.114	$1.64 \times 10^{-06}$		$8.98 \times 10^{+07}$	$\alpha$
$^{282}\text{Mc}$	11.617	$1.09 \times 10^{-03}$		$8.65 \times 10^{+04}$	$\alpha$
$^{278}\text{Nh}$	11.057 (11.60)	$6.61 \times 10^{-03}$	$2.77 \times 10^{-04}$	$1.33 \times 10^{+02}$	$\alpha$

**Table 6** continued

Nuclei	$Q_{\alpha}^{RMF}$	$T_{1/2}^{\alpha}$		$T_{1/2}^{SF}$	Mode of decay
		CPPM ( RMF $Q_{\alpha}$ )	CPPM (expt. $Q_{\alpha}$ )		
$^{274}\text{Rg}$	10.975(11.15)	$2.36 \times 10^{-03}$	$8.33 \times 10^{-04}$	$1.01 \times 10^{+02}$	$\alpha$
$^{270}\text{Mt}$	10.282(10.03)	$3.77 \times 10^{-02}$	0.199806	$4.68 \times 10^{+01}$	$\alpha$
$^{266}\text{Bh}$	8.901	137.725		$3.12 \times 10^{+01}$	SF
$^{262}\text{Db}$	8.132	13740.4		$8.89 \times 10^{+01}$	SF
$^{258}\text{Lr}$	7.446	$1.22 \times 10^{+06}$		$4.48 \times 10^{+03}$	SF
$^{291}\text{119}$	14.378	$1.72 \times 10^{-08}$		$2.01 \times 10^{+11}$	$\alpha$
$^{287}\text{Ts}$	13.071	$1.95 \times 10^{-06}$		$1.17 \times 10^{+08}$	$\alpha$
$^{283}\text{Mc}$	11.57	$1.38 \times 10^{-03}$		$1.33 \times 10^{+05}$	$\alpha$
$^{279}\text{Nh}$	10.712	0.053809		$2.14 \times 10^{+02}$	$\alpha$
$^{275}\text{Rg}$	10.962	$2.45 \times 10^{-03}$		$5.86 \times 10^{+01}$	$\alpha$
$^{271}\text{Mt}$	10.32	$2.83 \times 10^{-02}$		$9.11 \times 10^{+01}$	$\alpha$
$^{267}\text{Bh}$	8.729	525.71		$5.45 \times 10^{+01}$	SF
$^{263}\text{Db}$	7.786	313269.0		$1.00 \times 10^{+02}$	SF
$^{259}\text{Lr}$	7.334	$3.59 \times 10^{+06}$		$2.47 \times 10^{+03}$	SF
$^{292}\text{119}$	14.45	$1.22 \times 10^{-08}$		$4.05 \times 10^{+11}$	$\alpha$
$^{288}\text{Ts}$	13.081	$1.79 \times 10^{-06}$		$2.39 \times 10^{+08}$	$\alpha$
$^{284}\text{Mc}$	11.552	$1.47 \times 10^{-03}$		$3.07 \times 10^{+05}$	$\alpha$
$^{280}\text{Nh}$	10.486	0.221739		$2.65 \times 10^{+02}$	$\alpha$
$^{276}\text{Rg}$	10.434	0.063858		$3.98 \times 10^{+01}$	$\alpha$
$^{272}\text{Mt}$	10.56	$5.93 \times 10^{-03}$		$1.42 \times 10^{+02}$	$\alpha$
$^{268}\text{Bh}$	8.804	276.127		$1.24 \times 10^{+02}$	SF
$^{264}\text{Db}$	7.442	$8.68 \times 10^{+06}$		$1.90 \times 10^{+02}$	SF
$^{260}\text{Lr}$	7.144	$2.46 \times 10^{+07}$		$2.85 \times 10^{+03}$	SF

$$a, b, c = \begin{cases} -25.31, -1.1629, 1.5864 & \text{even - even;} \\ -26.65, -1.0859, 1.5848 & \text{even - odd;} \\ -25.68, -1.1423, 1.5920 & \text{odd - even;} \\ -29.48, -1.1130, 1.6971 & \text{odd - odd.} \end{cases} \tag{27}$$

Recently, in Ref. [40] Ni et al. proposed a unified formula for determining the half-lives in alpha decay and cluster radioactivity. The formula for alpha decay is written as

$$\log_{10} T_{1/2}^{\alpha} = 2a\sqrt{\mu}(Z - 2)Q_{\alpha}^{-1/2} + b\sqrt{\mu}[2(Z - 2)]^{-1/2} + c \tag{28}$$

where  $a, b, c$  are the constants and  $\mu$  is defined as  $4(A-4)/A$ .

### 3.5.2 Beta decay

Beta decay, a three-body decay mode, is another very important mode of decay for the nuclei lie far from the stability line. The description of  $\beta$ -decay is explained by famous Fermi theory which describes the beta transition rates according to  $\log(ft)$  values. It proceeds through weak interaction, and this process is slow as well as less favoured compared to SF and alpha decay. Recently, it is predicted that there may also be a possibility of  $\beta$ -decay in some of the superheavy nuclei where it may play a significant role [110]. In this regard, even in the presence of dominant mode of alpha and SF in SHN, we make the search for possibility of  $\beta$ -decay in order to completeness of decay modes of superheavy nuclei. To look out the possibility of  $\beta$ -decay in considered isotopic chain, we employed the empirical formula of Fiset and Nix [109] for estimating the half-lives of the isotopic chain under study which is given by

$$T_{1/2}^{\beta} = 540 \times 10^{5.0} \frac{m_e^5}{\rho_{d.o.s.}(W_{\beta}^6 - m_e^6)}. \tag{29}$$

**Table 7** CPPM study of  $\alpha$ -decay chains of fission survival nuclides (i.e.  $^{293-297}119$ ). Experimental data for  $Q_\alpha$  [105–107], if available, are given in parentheses with asterisk

Nuclei	$Q_\alpha^{RMF}$	$T_{1/2}^\alpha$		$T_{1/2}^{SF}$	Mode of decay
		CPPM (RMF $Q_\alpha$ )	CPPM (expt. $Q_\alpha$ )		
$^{293}119$	15.317	$3.25 \times 10^{-10}$		$2.37 \times 10^{+11}$	$\alpha$
$^{289}\text{Ts}$	12.984	$2.77 \times 10^{-06}$		$1.38 \times 10^{+08}$	$\alpha$
$^{285}\text{Mc}$	11.603	$1.05 \times 10^{-03}$		$2.24 \times 10^{+05}$	$\alpha$
$^{281}\text{Nh}$	10.317	0.65282		$2.20 \times 10^{+02}$	$\alpha$
$^{277}\text{Rg}$	10.169	0.353285		$1.05 \times 10^{+01}$	$\alpha$
$^{273}\text{Mt}$	10.508	$7.91 \times 10^{-03}$		$4.19 \times 10^{+01}$	$\alpha$
$^{269}\text{Bh}$	8.814	245.475		$8.66 \times 10^{+01}$	SF
$^{265}\text{Db}$	6.833	$5.86 \times 10^{+09}$		$1.34 \times 10^{+02}$	SF
$^{294}119$	15.131	$6.68 \times 10^{-10}$		$2.27 \times 10^{+11}$	$\alpha$
$^{290}\text{Ts}$	12.956	$3.07 \times 10^{-06}$		$1.55 \times 10^{+08}$	$\alpha$
$^{286}\text{Mc}$	11.561	$1.29 \times 10^{-03}$		$2.63 \times 10^{+05}$	$\alpha$
$^{282}\text{Nh}$	10.188	1.5027		$2.93 \times 10^{+02}$	$\alpha$
$^{278}\text{Rg}$	9.925	1.80751		$3.98 \times 10^{+00}$	$\alpha$
$^{295}119$	16.177	$1.17 \times 10^{-11}$		$4.59 \times 10^{+10}$	$\alpha$
$^{291}\text{Ts}$	11.763	$1.69 \times 10^{-03}$		$5.10 \times 10^{+07}$	$\alpha$
$^{287}\text{Mc}$	11.332 (10.74)	$4.75 \times 10^{-03}$	0.183249	$9.51 \times 10^{+04}$	$\alpha$
$^{283}\text{Nh}$	10.097(10.26)	2.70304	0.887961	$1.37 \times 10^{+02}$	$\alpha$
$^{279}\text{Rg}$	9.666 (10.52)	10.9634	0.032815	$7.76 \times 10^{-01}$	SF
$^{296}119$	16.017	$2.02 \times 10^{-11}$		$1.71 \times 10^{+10}$	$\alpha$
$^{292}\text{Ts}$	11.596	$4.27 \times 10^{-03}$		$2.82 \times 10^{+07}$	$\alpha$
$^{288}\text{Mc}$	11.262 (10.46)	$6.94 \times 10^{-03}$	1.10276	$6.34 \times 10^{+04}$	$\alpha$
$^{284}\text{Nh}$	9.920(10.00)	8.99101	5.11525	$1.06 \times 10^{+02}$	$\alpha$
$^{280}\text{Rg}$	9.454 (9.75)	50.3186	5.7732	$5.10 \times 10^{-01}$	SF

In an analogy of  $\alpha$ -decay, we evaluate the  $Q_\beta$  value using the relation  $Q_\beta = BE(Z + 1, A) - BE(Z, A)$  and further we calculate the  $W_\beta$  by a relation  $W_\beta = Q_\beta + m_e$ , where  $m_e$  is the rest mass of electron. Here,  $\rho_{d.o.s.}$  is the average density of states in the daughter nucleus ( $e^{-A/290} \times$  number of states within 1 MeV of ground state).

### 3.5.3 Spontaneous fission

Superheavy nuclei are identified by alpha decay and the chain ends by spontaneous fission which helps in identifying the long-lived superheavy elements. Several empirical formulas for determining the spontaneous fission half-lives are available in the literature proposed by various authors from time to time.

**Ren and Xu** In our calculations, we employed the phenomenological formula proposed by Ren and Xu [58] expressed as

$$\log_{10} T_{1/2}^{SF} = 21.08 + C_1 \frac{(Z - 90 - \nu)}{A} + C_2 \frac{(Z - 90 - \nu)^2}{A} + C_3 \frac{(Z - 90 - \nu)^3}{A} + C_4 \frac{(Z - 90 - \nu)(N - Z - 52)^2}{A}, \tag{30}$$

where  $Z, N, A$  represent the proton, neutron and mass number of parent nuclei.  $C_1, C_2, C_3, C_4$  are the empirical constants and  $\nu$  is the seniority term which takes care of blocking effect of unpaired nucleons on the transfer of many nucleon pairs during the fission process.

*Santhosh et al.* Spontaneous fission (SF) was first described within the geometrical framework of the charged liquid drop model by Bohr and Wheeler [48]. The first semi-empirical formula for finding the half-lives of SF was proposed by Swiatecki [50] and showed that this formula can reproduce experimental values reasonably. The quantum tunnelling effect is considered as the underlying mechanism of SF and the probability of tunnelling depends exponentially on the square root of the barrier height and inversely proportional to the fissionability parameter  $\frac{Z^2}{A}$ . A semi-empirical formula for SF half-lives [111] was developed by



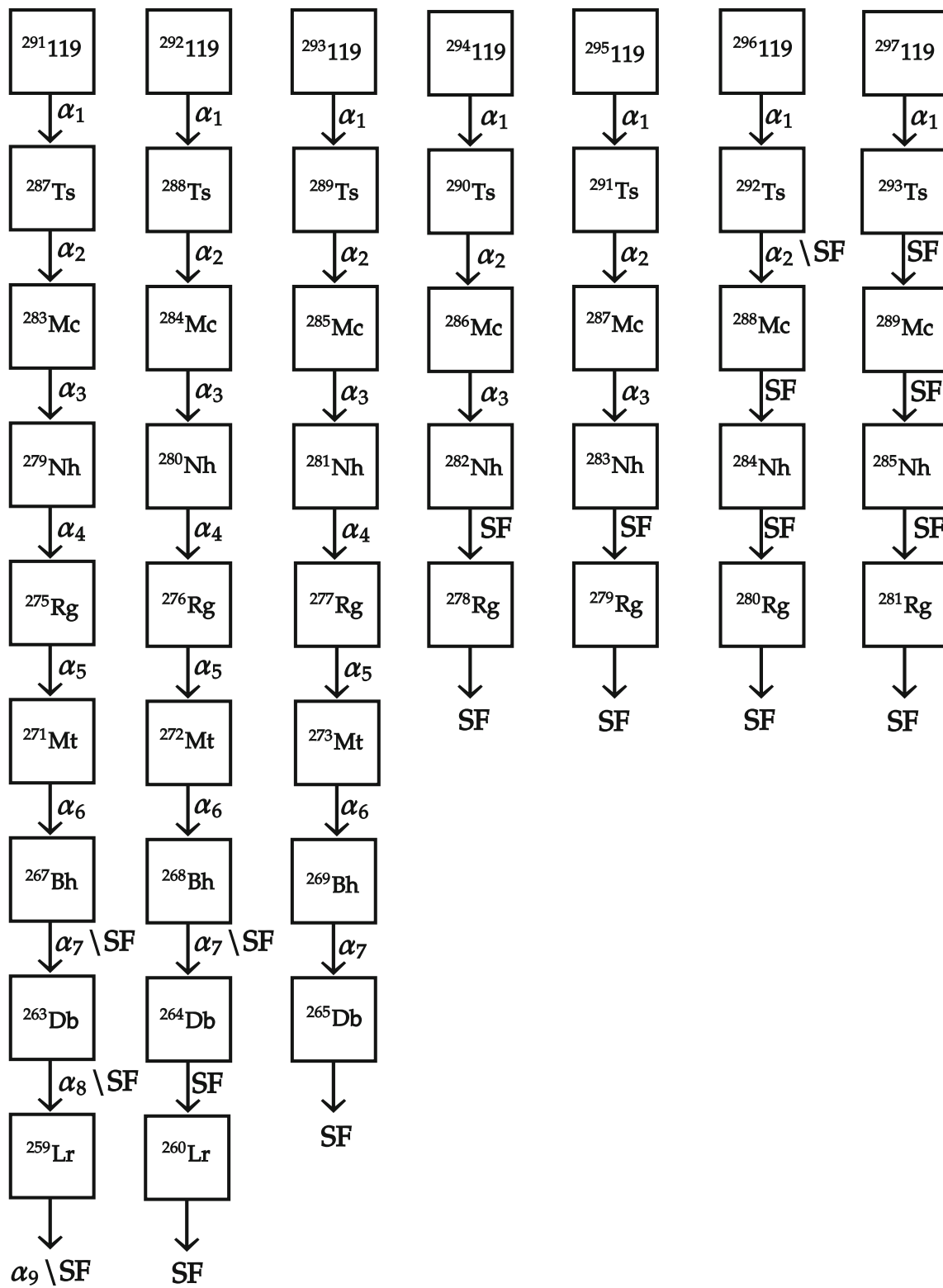
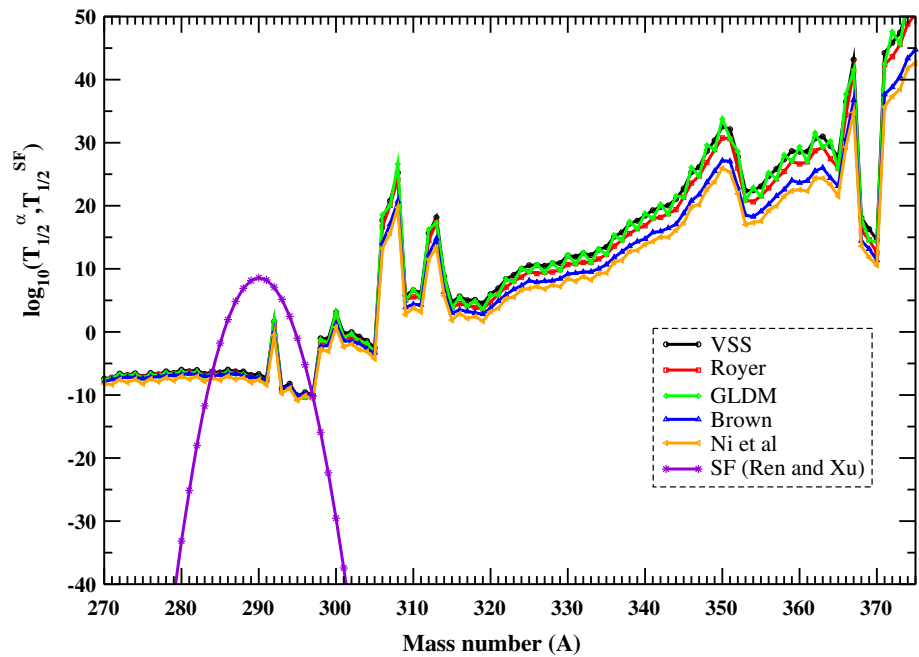


Fig. 6 Decay chain of  $^{291-297}_{119}$

**Fig. 7** Alpha decay and spontaneous fission half-lives of  $Z = 119$  isotopic chain as a function of mass number



including fissionability parameter and isospin effect  $\frac{N-Z}{N+Z}$ . Later this formula was modified [112] by incorporating shell correction term, as shell structure plays an important role in determining SF half-lives and is given as

$$\log_{10} T_{1/2}^{SF} = a \frac{Z^2}{A} + b \left( \frac{Z^2}{A} \right)^2 + c \left( \frac{N-Z}{N+Z} \right) + d \left( \frac{N-Z}{N+Z} \right)^2 + e E_{shell} + f \tag{31}$$

where  $a = -43.25203$ ,  $b = 0.49192$ ,  $c = 3674.3927$ ,  $d = -9360.6$ ,  $e = 0.8930$  and  $f = 578.56058$ .  $E_{shell}$  is the shell correction energy taken from Ref. [113].

We have studied the modes of decay of superheavy nuclei  $^{284-296}_{119}$  and their daughters in the alpha decay chains by comparing SF half-lives with corresponding alpha half-lives. The SF half-lives are computed using the formula of Santhosh et al [112] and alpha half-lives computed using CPPM [75, 76]. For computing alpha half-lives  $Q$  values obtained using RMF formalism and in few cases available experimental  $Q$  values are used. The nuclei with alpha half-life less than SF half-life will undergo alpha decay and vice versa. The entire results of our calculations are given in Tables 5, 6 and 7. From these table it can be seen that our alpha half-life values computed using  $Q_{\alpha}$ (RMF) agree with half-life values computed using experimental  $Q_{\alpha}$  values within 1 order difference. Also it can be seen that the isotopes  $^{288-293}_{119}$  exhibit consistent 6  $\alpha$  chains followed by SF,  $^{294}_{119}$  isotopes show 5 consistent  $\alpha$  chains,  $^{295,296}_{119}$  exhibit consistent 4 chains followed by SF and the rest of the nuclei show continuous alpha chains. The isotopes  $^{288-293}_{119}$ ,  $^{295,296}_{119}$  will be of great interest to experimentalists for future studies.

Present analysis shows that some of the isotopes of  $Z = 119$  superheavy nuclei survived the fission and thus make the decay via  $\alpha$ -emission. The calculated  $\alpha$ -decay half-lives using VSS, Brown, Royer, GLDM and Ni et al. are framed in Tables 2, and we noticed a good agreement among them as well as with FRDM data. Fiset and Nix formula is employed to calculate the  $\beta$ -decay half-life for examining the possibility of mode of  $\beta$ -decay, and the results are also presented in Tables 2. It is noted that  $\beta$ -decay half-lives are found to be large than  $\alpha$ -decay as well as spontaneous fission half-lives and hence there is no possibility of mode of  $\beta$ -decay observed for current isotopic chain. Spontaneous fission half-lives are calculated using Ren and Xu formula, and the estimated values are presented in one of the columns of Tables 2, 3, 4. The calculated half-lives for  $\alpha$ -decay and SF are plotted against the mass number in Fig. 7.

Our calculations based on RMF predict that the nuclides  $^{284-296}_{119}$  survive the fission and may be observed in the laboratory through alpha decay and the nuclei beyond  $A > 296$  do not survive fission and hence completely undergo spontaneous fission. Further, we aimed at predicting the possibility of  $\alpha$ -decay chain of fission survival nuclides, i.e.  $^{284-296}_{119}$  of the considered isotopic chain given in Tables 3 and 4. Our study confirmed the possibility of one  $\alpha$  chain from  $^{284,296}_{119}$ , two consistent  $\alpha$  chains from  $^{285,295}_{119}$ , three consistent  $\alpha$  chains from  $^{286,294}_{119}$ , four consistent  $\alpha$  chains from  $^{287}_{119}$ , six consistent alpha chains from  $^{288-293}_{119}$ , and these findings are reported in Table 3 and 4. The  $\alpha$ -decay chains of fission surviving nuclides  $^{284-296}_{119}$  are pictorially shown in figures 5 and 6. Unfortunately, there is no experimental information for  $Z = 119$  nuclides. But the experimental data of  $Q_{\alpha}$  for a few decay isotopes of  $Z = 119$  are available [105–107] and are mentioned in Tables 3 and 4. The calculated values of  $Q_{\alpha}$  are compared with available experimental data [105–107], and we found a close agreement between them. Moreover, the  $\alpha$ -decay chain of  $^{295}_{119}$  contains  $^{291}\text{Ts}$ ,  $^{287}\text{Mc}$ ,  $^{283}\text{Nh}$  and  $^{279}\text{Rg}$  elements whose  $\alpha$ -decay chain is treated in Refs. [87, 114] and a close agreement of our calculated  $Q_{\alpha}$  with the values predicted in these Refs. [87, 114] is noticed. However, we did not mention the values of  $Q_{\alpha}$  predicted

in Refs. [87, 114] into the manuscript. The inference drawn from this investigations is that the nuclides  $^{284-296}_{119}$  have the  $\alpha$ -decay chain with the life time of the order of micro- or nano-second and thus these nuclides might be observed in the laboratory through alpha decay. We firmly believed that the alpha decay life time of the isotopes  $^{284-296}_{119}$  presented in the manuscript may serve as a crucial theoretical input for designing the experimental setup and might provide a ray of hope in order to produce the yet-to-be synthesized isotopes of  $Z = 119$  in the laboratory in very near future.

#### 4 Summary and conclusion

In summary, we have calculated the structural properties of  $Z = 119$  superheavy nuclei within a mass range  $284 \leq A \leq 375$  using axially deformed relativistic mean field model. The calculations are performed for three different shape configurations prolate, oblate and spherical configurations in which prolate is suggested to be possible ground state for most of the nuclei. Binding energy produced by RMF is in good agreement with FRDM data. Two-dimensional contour plot of density distribution has been made for predicting neutron shell closure nuclides  $^{291}_{119}$  and  $^{303}_{119}$  to reveal the special features of the nuclei such as bubble or cluster structures. Further, the predictions of possible modes of decay such as  $\alpha$ -decay,  $\beta$ -decay and spontaneous fission of the isotopic chain of  $Z = 119$  in the mass range  $284 \leq A \leq 375$  have been made. The calculations performed for  $\alpha$  decay half-lives using the semi-empirical formulae Viola-Seaborg, Brown, Royer, GLDM and Ni et al. are in good agreement with among each other as well as with macro-microscopic FRDM data wherever available. In addition, a thorough study on  $\beta$ -decay and SF half-lives has also been made to identify the mode of the decay of these isotopes. We conclude that the  $\alpha$ -decay and spontaneous fission are the principal modes of decay in considered chain of nuclides and there is no possibility of  $\beta$ -decay for the considered chain of nuclides under study. The calculated values of  $Q_\alpha$  are compared with experimental data [105–107], wherever available and found a close agreement between them. Moreover, our calculated  $Q_\alpha$  are in good agreement with the values predicted in Refs. [87, 114].

From our analysis we inferred that the isotopes with mass number  $284 \leq A \leq 296$  will survive fission and can be observed in the laboratory through alpha decay while beyond the mass number  $A > 296$  do not survive fission and hence completely undergo spontaneous fission. We also analysed the  $\alpha$ -decay chain of fission survival nuclides, i.e.  $^{284-296}_{119}$  for the considered isotopic chain, and predicted one  $\alpha$  decay chain for  $^{284,296}_{119}$  followed by SF, two consistent  $\alpha$  decay chains for  $^{285,295}_{119}$ , three consistent  $\alpha$  decay chains for  $^{286,294}_{119}$ , four consistent  $\alpha$  decay chains for  $^{287}_{119}$  and six consistent  $\alpha$  decay chains for  $^{288-293}_{119}$ . Findings on  $\alpha$ -decay chain suggest that the nuclides  $^{284-296}_{119}$  have  $\alpha$ -decay chain with the life time of the order of micro- or nano-second, and thus, these isotopes might be observed in the laboratory through alpha decay. Moreover, the SF half-life and alpha decay half-life for the isotopic chain  $^{284-296}_{119}$  are estimated by the formula of Santosh et al and by CPPM, respectively. These investigations showed that the isotopic chain  $^{288-293}_{119}$  exhibits 6  $\alpha$  consistent chains followed by SF, the isotopes  $^{295,296}_{119}$  undergo 4  $\alpha$  decays followed by SF, and the rest of the isotopes undergo consistent alpha decays. Both axially deformed relativistic mean field model and CPPM by Santosh et al predict 6  $\alpha$  consistent chains for the isotopic chain  $^{288-293}_{119}$  and thus are in very good agreement with each other.

The isotopes  $^{288-293}_{119}$  and  $^{295,296}_{119}$  may prove to be of significant interest to experimentalists for future studies. Thus, we hope that these predictions on the possible decay modes of  $Z = 119$  superheavy nuclei might prove to be quite useful and may serve as a significant input for future experimental investigations.

**Acknowledgements** One of the authors Asloob A. Rather would like to acknowledge Dashty T. Akrawy, Researcher at Physics Department, College of Science, Salahaddin University, Erbil 44001, Kurdistan, Iraq, for careful reading of the manuscript and constructive criticism. Asloob A. Rather will also like to express his gratitude to Dorin N. Poenaru, Senior Scientist at Horia Hulubei National Institute of Physics and Nuclear Engineering (IFIN-HH), P.O. Box MG-6, RO-077125 Bucharest-Magurele, Romania, for his valuable comments on the write-up and encouragement.

**Data Availability Statement** There are no data available in the manuscript.

#### References

1. S.C. Cwiok, J. Dobaczewski, P.-H. Heenen, P. Magierski, W. Nazarewicz, Nucl. Phys. A **611**, 211 (1996)
2. W.D. Myers, W.J. Swiatecki, Nucl. Phys. A **81**, 1 (1966)
3. A. Sobczewski, F.A. Gareev, B.N. Kalinkin, Phys. Lett. **22**, 500 (1966)
4. U. Mosel, W. Greiner, Z. Phys. **222**, 261 (1969)
5. S.C. Cwiok, V.V. Pashkevich, J. Dudek, W. Nazarewicz, Nucl. Phys. A **41**, 254 (1983)
6. Z. Patyk, A. Sobczewski, Nucl. Phys. A **533**, 132 (1991)
7. S. Hoffman, G. Munzenberg, Rev. Mod. Phys. **72**, 733 (2000)
8. Yu. Ts. Oganessian. J. Phys. G Nucl. Part. Phys. **34**, R165 (2007)
9. S. Hofmann, F.P. Heßberger, D. Ackermann, S. Antalic, P. Cagarda, B. Kindler, P. Kuusiniemi, M. Leino, B. Lommel, O.N. Malyshev, R. Mann, G. Munzenberg, A.G. Popeko, S. Saro, B. Streicher, A.V. Yeremin, Nucl. Phys. A **734**, 93 (2004)
10. D. Ackermann, Nucl. Phys. A **787**, 353c (2007)
11. K. Morita, Nucl. Phys. A **944**, 30 (2015)
12. Yu. Ts. Oganessian, V.K. Utyonkov, Rep. Prog. Phys. **78**, 036301 (2015)
13. Yu. Ts. Oganessian et al., Phys. Rev. C **79**, 024603 (2009)



14. Yu Ts. Oganessian et al., *Phys. Rev. Lett.* **109**, 162501 (2012)
15. Yu. Ts. Oganessian et al., *JINR Communication No. E7-2012-58*, (2012)
16. J.C. Pei, F.R. Xu, Z.J. Lin, E.G. Zhao, *Phys. Rev. C* **76**, 044326 (2007)
17. M.M. Sharma, A.R. Farhan, G. Munzenberg, *Phys. Rev. C* **71**, 054310 (2005)
18. W.D. Myers, W.J. Swiatecki, *Ark. Fys.* **36**, 343 (1967)
19. H. Meldner, *Ark. Fys.* **36**, 593 (1967)
20. S.G. Nilsson, C.F. Tsang, A. Sobiczewski, Z. Szymanski, S. Wycech, C. Gustafson, I.L. Lamm, P. Möller, B. Nilsson, *Nucl. Phys. A* **131**, 1 (1969)
21. M. Bender, K. Rutz, P.G. Reinhard, J.A. Maruhn, W. Greiner, *Phys. Rev. C* **58**, 2126 (1998)
22. K. Rutz, M. Bender, T. Burvenich, T. Schilling, P.G. Reinhard, J.A. Maruhn, W. Greiner, *Phys. Rev. C* **56**, 238 (1997)
23. T. Sil, S.K. Patra, B.K. Sharma, M. Centelles, X. Viñas, *Phys. Rev. C* **69**, 044315 (2004)
24. S. Cwiok, W. Nazarewicz, P.H. Heenen, *Phys. Rev. Lett.* **83**, 1108 (1999)
25. J. Dong, W. Zuo, W. Scheid, *Phys. Rev. Lett.* **107**, 012501 (2011)
26. D.N. Poenaru, R.A. Gherghescu, W. Greiner, *Phys. Rev. Lett.* **107**, 062503 (2011)
27. E. Rutherford, H. Geiger, *Proc. R. Soc. Lond. Ser. A* **81**, 162 (1908)
28. E. Rutherford, T. Royds, *Philos. Mag.* **17**, 281 (1909)
29. G. Gamow, *Z. Phys.* **51**, 204 (1928)
30. B. Buck, A.C. Merchant, S.M. Perez, *Phys. Rev. C* **45**, 2247 (1992)
31. D.N. Poenaru, M. Ivascu, A. Sandalescu, W. Greiner, *Phys. Rev. C* **32**, 572 (1985)
32. D.N. Basu, *Phys. Lett. B* **566**, 90 (2003)
33. H.F. Zhang, G. Royer, *Phys. Rev. C* **76**, 047304 (2007)
34. Y.Z. Wang, S.J. Wang, Z.Y. Hou, J.Z. Gu, *Phys. Rev. C* **92**, 064301 (2015)
35. Asloob A. Rather, M. Ikram, A.A. Usmani, Bharat Kumar, S.K. Patra, *Eur. Phys. J. A* **52**, 372 (2016)
36. V.E. Viola Jr., G.T. Seaborg, *J. Inorg. Nucl. Chem.* **28**, 741 (1966)
37. B.A. Brown, *Phys. Rev. C* **46**, 811 (1992)
38. G. Royer, *J. Phys. G, Nucl. Part. Phys.* **26**, 1149 (2000)
39. N. DasguptaSchubert, M.A. Reyes, *At. Data Nucl. Data Tables* **93**, 90 (2007)
40. D.D. Ni, Z. Ren, T.K. Dong et al., *Phys. Rev. C* **78**, 044310 (2008)
41. N. Wang, M. Liu, X.Z. Wu, J. Meng, *Phys. Lett. B* **734**, 215 (2014)
42. D.N. Poenaru, R.A. Gherghescu, N. Carjan, *EPL* **77**, 62001 (2007)
43. V.E. Viola Jr., G.T. Seaborg, *J. Inorg. Nucl. Chem.* **28**, 741 (1966)
44. A. Sobiczewski, Z. Patyk, S.C. Cwiok, *Phys. Lett. B* **224**, 1 (1989)
45. A. Sobiczewski, A. Parkhomenko, *Prog. Part. Nucl. Phys.* **58**, 292 (2007)
46. A. Parkhomenko, A. Sobiczewski, *Acta Phys. Pol. B* **36**, 3095 (2005)
47. D. Ni, Z. Ren, T. Dong, C. Xu, *Phys. Rev. C* **78**, 044310 (2008)
48. N. Bohr, J.A. Wheeler, *Phys. Rev.* **56**, 426 (1939)
49. G.N. Flerov, K.A. Petrjak, *Phys. Rev.* **58**, 89 (1940)
50. W.J. Swiatecki, *Phys. Rev.* **100**, 937 (1955)
51. Yu Ts.. Oganessian et al., *Phys. Rev. C* **72**, 034611 (2005)
52. Yu.. Ts. Oganessian et al., *Phys. Rev. C* **74**, 044602 (2006)
53. K.E. Gregorich, J.M. Gates, Ch.E. Dullmann, R. Sudowe, S.L. Nelson, M.A. Garcia, I. Dragojević, C.M. Folden III., S.H. Neumann, D.C. Hoffman, H. Nitsche, *Phys. Rev. C* **74**, 044611 (2006)
54. J. Dvorak et al., *Phys. Rev. Lett.* **97**, 242501 (2006)
55. D. Peterson et al., *Phys. Rev. C* **74**, 014316 (2006)
56. Yu. Oganessian et al., *Phys. Rev. C* **70**, 064609 (2004)
57. C. Xu, Z. Ren, Y. Guo, *Phys. Rev. C* **78**, 044329 (2008)
58. Z. Ren, C. Xu, *Nucl. Phys. A* **759**, 64 (2005)
59. C. Xu, Z. Ren, *Phys. Rev. C* **71**, 014309 (2005)
60. R. Smolanczuk, J. Skalski, A. Sobiczewski, *Phys. Rev. C* **52**, 1871 (1995)
61. I. Muntain, Z. Patyk, A. Sobiczewski, *Acta Phys. Pol. B* **34**, 2141 (2003)
62. M. Warda, J.L. Egido, *Phys. Rev. C* **86**, 014322 (2012)
63. A. Staszczak, A. Baran, W. Nazarewicz, *Phys. Rev. C* **87**, 024320 (2013)
64. W. Pannert, P. Ring, J. Boguta, *Phys. Rev. C* **59**, 2420 (1987)
65. B.D. Serot, *Rep. Prog. Phys.* **55**, 1855 (1992)
66. Y.K. Gambhir, P. Ring, A. Thimet, *Ann. Phys. N. Y.* **198**, 132 (1990)
67. P. Ring, *Prog. Part. Nucl. Phys.* **37**, 193 (1996)
68. B.D. Serot, J.D. Walecka, *Adv. Nucl.* **16**, 1 (1986)
69. J. Boguta, A.R. Bodmer, *Nucl. Phys. A* **292**, 413 (1977)
70. S.K. Patra, C.R. Prahara, *Phys. Rev. C* **44**, 2552 (1991)
71. Z. Ren, D.H. Chen, F. Tai, H.Y. Zhang, W.Q. Shen, *Phys. Rev. C* **76**, 064302 (2003)
72. M.M. Sharma, A.R. Farhan, *Phys. Rev. C* **71**, 054310 (2005)
73. D.G. Madland, R.J. Nix, *Nucl. Phys. A* **476**, 1 (1988)
74. G.A. Lalazissis, S. Karatzikos, R. Fossion, D. Pena Arteaga, A.V. Afanasjev, P. Ring, *Phys. Lett.* **671**, 36 (2009)
75. K.P. Santhosh, A. Joseph, *Pramana* **55**, 375 (2000)
76. K.P. Santhosh, R.K. Biju, S. Sahadevan, A. Joseph, *Phys. Scr.* **77**, 065201 (2008)
77. K.P. Santhosh, R.K. Biju, S. Sahadevan, *J. Phys. G Nucl. Part. Phys.* **36**, 115101 (2009)
78. K.P. Santhosh, S. Sahadevan, R.K. Biju, *Nucl. Phys. A* **825**, 159 (2009)
79. J. Blocki, J. Randrup, W.J. Swiatecki, C.F. Tsang, *Ann. Phys. N. Y.* **105**, 427 (1977)
80. J. Blocki, W.J. Swiatecki, *Ann. Phys. N. Y.* **132**, 53 (1981)
81. Yu. Oganessian et al., *Phys. Rev. Lett.* **74**, 044602 (2006)
82. Yu Ts. Oganessian, *J. Phys. G Nucl. Part. Phys.* **34**, R165 (2007)
83. Z.H. Liu, J.D. Bao, *Phys. Rev. C* **80**, 054608 (2009)

84. N. Ghahramany, A. Ansari, *Eur. Phys. J. A* **52**, 287 (2016)
85. N. Wang, E.G. Zhao, W. Schield, S.G. Zhou, *Phys. Rev. C* **85**, 041601(R) (2012)
86. L. Zhu, W.J. Xie, F.S. Zhang, *Phys. Rev. C* **89**, 024615 (2014)
87. G.G. Adamian, N.V. Antoneko, H. Lenske, *Nucl. Phys. A* **970**, 22 (2018)
88. G.Z. Guo, Z.X. Hong, H.M. Hui, F.Z. Qing, L.J. Qing, *Sci. China* **54**, s61 (2011)
89. P. Moller, J.R. Nix, W.D. Wyers, W.J. Swiatecki, *At. Data Nucl. Data Tables* **59**, 185 (1999)
90. P. Moller, J.R. Nix, K.L. Kratz, *At. Data Nucl. Data Tables* **66**, 131 (1997)
91. H. Morinaga, *Phys. Rev.* **101**, 254 (1956)
92. P. Van Duppen, E. Coenen, K. Deneffe, M. Huyse, K. Heyde, P. Van Isacker, *Phys. Rev. Lett.* **52**, 1974 (1984)
93. A.N. Andreyev et al., *Nature* **405**, 430 (2000)
94. Z. Ren, *Phys. Rev. C* **65**, 051304(R) (2002)
95. Z. Shi-Jie, X. Fu-Rong, *Chin. Phys. C* **32**, 42 (2008)
96. Z.X. Li, Z.H. Zhang, P.W. Zhao, *Front. Phys.* **10**, 102101 (2015)
97. S. Ćwiok, P.H. Heenen, W. Nazarewicz, *Nature* **433**, 705 (2000)
98. Z. Ren, H. Toki, *Nucl. Phys.* **689**, 691 (2001)
99. J. A. Wheeler (unpublished)
100. H.A. Wilson, *Phys. Rev. C* **69**, 538 (1946)
101. J. Decharge et al., *Nucl. Phys. A* **716**, 55 (2003)
102. M. Grasso et al., *Phys. Rev. C* **79**, 034318 (2009)
103. S.K. Singh, M. Ikram, S.K. Patra, *Int. J. Mod. Phys. E* **22**, 1350001 (2013)
104. B.K. Sharma, P. Arumugam, S.K. Patra, P.D. Stevenson, R.K. Gupta, W. Greiner, *Phys. G Nucl. Part. Phys.* **32**, L1 (2006)
105. Yu. Ts. Oganessian, *J. Phys. G* **34**, R165 (2007)
106. Yu Ts. Oganessian, *Phys. Rev. C* **87**, 014302 (2013)
107. J.H. Hamilton, Yu Ts. Oganessian, V.K. Utyonkov et al., *J. Phys. G Conf. Ser.* **403**, 012035 (2012)
108. G. Audi, A.H. Wapstra, C. Thibault, *Nucl. Phys. A* **729**, 337 (2003)
109. E.O. Fiset, J.R. Nix, *Nucl. Phys. A* **193**, 647 (1972)
110. A.V. Karpov, V.I. Zagrebaev, Y.M. Palenzeula, L.F. Ruiz, W. Greiner, *Int. J. Mod. Phys. E* **21**, 1250013 (2012)
111. K.P. Santhosh, R.K. Biju, S. Sabina, *Nucl. Phys. A* **832**, 220 (2010)
112. K.P. Santhosh, C. Nithya, *Phys. Rev. C* **94**, 054621 (2016)
113. P. Möller, A.J. Sierk, T. Ichikawa, H. Sagawa, *At. Data Nucl. Data Tables* **109**, 1 (2016)
114. A.N. Kuzmina, G.G. Adamian, N.V. Antonenko, *Phys. Rev. C* **85**, 017302 (2012)

Springer Nature or its licensor (e.g. a society or other partner) holds exclusive rights to this article under a publishing agreement with the author(s) or other rightsholder(s); author self-archiving of the accepted manuscript version of this article is solely governed by the terms of such publishing agreement and applicable law.